

Characterization, Estimation, and Mitigation of Interference in Multi-Radio Multi-Channel Wireless Mesh Networks

Srikant Manas Kala

A Thesis Submitted to
Indian Institute of Technology Hyderabad
In Partial Fulfillment of the Requirements for
The Degree of Master of Technology



Department of Computer Science and Engineering

June 2015

Declaration

I declare that this written submission represents my ideas in my own words, and where ideas or words of others have been included, I have adequately cited and referenced the original sources. I also declare that I have adhered to all principles of academic honesty and integrity and have not misrepresented or fabricated or falsified any idea/data/fact/source in my submission. I understand that any violation of the above will be a cause for disciplinary action by the Institute and can also evoke penal action from the sources that have thus not been properly cited, or from whom proper permission has not been taken when needed.

Manas Kala

(Signature)

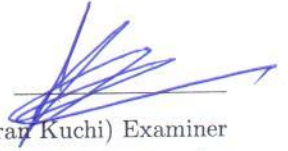
(Srikant Manas Kala)

CS12M1012

(Roll No.)

Approval Sheet

This Thesis entitled Characterization, Estimation, and Mitigation of Interference in Multi-Radio Multi-Channel Wireless Mesh Networks by Srikant Manas Kala is approved for the degree of Master of Technology from IIT Hyderabad



(Dr. Kiran Kuchi) Examiner
Dept. of Electrical Engineering
IITH



(Dr. Antony Franklin) Examiner
Dept. of Computer Science and Engineering
IITH



(Dr. Bheemarjuna Reddy Tamma) Adviser
Dept. of Computer Science and Engineering
IITH



(Dr. Kotaro Kataoka) Chairman
Dept. of Computer Science and Engineering
IITH

Acknowledgements

I am profoundly grateful to my thesis advisor Dr. Bheemarjuna Reddy Tamma for his constant help, unwavering support and learned guidance. I express my sincere appreciation for his encouragement and counsel that helped me carry out this research study. I extend my special thanks to Pavan Kumar Reddy M, Ranadheer Musham, Mukesh Giluka, Vanlin Sathya, Pavithra Muthyap and Hatim Lokhandwala for their help and inputs. I would also like to thank Dr. Naveen Sivadasan for introducing me to topics in algorithms which were of immense help in my work. Most importantly, I am forever grateful to my parents, Betty Lala and God for being my strength and anchor.

Dedication

I dedicate this thesis to my mother, and the countless children who lost their families on
June 16, 2013 in the Uttarakhand floods.

Abstract

Wireless Mesh Networks (WMNs) have evolved into a wireless communication technology of immense interest. But technological advancements in WMNs have inadvertently spawned a plethora of network performance bottlenecks, caused primarily by the rise in prevalent interference. The benefits that multi-radio multi-channel (MRMC) WMNs offer *viz.*, augmented network capacity, uninterrupted connectivity and reduced latency, are depreciated by the detrimental effect of prevalent interference. Interference mitigation is thus a prime objective in WMN deployments. Conflict Graphs are indispensable tools used to theoretically represent and estimate the interference in wireless networks. This interference is multi-dimensional, *radio co-location interference* (RCI) being a crucial aspect that is seldom addressed in conflict graph generation approaches suggested in research studies. Further, designing high performance channel assignment (CA) schemes to harness the potential of MRMC deployments in WMNs is an active research domain. A pragmatic channel assignment approach strives to maximize network capacity by restraining the endemic interference and mitigating its adverse impact on network performance metrics. However, numerous CA schemes have been proposed in research literature and there is a lack of CA performance prediction techniques which could assist in choosing a suitable CA for a given WMN.

This thesis proposes a generic algorithm to generate conflict graphs which is independent of the underlying interference model. It puts forward the notion of RCI, which is caused and experienced by spatially co-located radios in MRMC WMNs. We experimentally validate the concept, and propose a new all-encompassing algorithm to create a radio co-location aware conflict graph. The novel conflict graph generation algorithm is demonstrated to be significantly superior and more efficient than the conventional approach, through theoretical interference estimates and comprehensive experiments. The results of an extensive set of ns-3 simulations run on the IEEE 802.11g platform strongly indicate that the radio co-location aware conflict graphs are a marked improvement over their conventional counterparts.

Further, this thesis proposes a set of intelligent channel assignment algorithms that focus primarily on alleviating RCI. These graph theoretic schemes are structurally inspired by the spatio-statistical characteristics of interference. We present the theoretical design foundations for each of the proposed algorithms, and demonstrate their potential to significantly enhance network capacity in comparison to some existing well-known schemes. We also demonstrate the adverse impact of radio co-location interference on the network, and the efficacy of the proposed schemes in successfully mitigating it. The experimental results to validate the proposed theoretical notions were obtained by running an exhaustive set of ns-3 simulations in an IEEE 802.11g/n environment.

Finally, this study questions the use of *total interference degree* (TID) as a reliable metric to predict the performance of a channel assignment scheme in a given WMN deployment. We offer a fresh characterization of the interference endemic in wireless networks. We then propose a reliable CA performance prediction metric, which employs a statistical interference estimation approach and could aid in the selection of an efficient CA scheme for a given WMN. We carry out a rigorous quantitative assessment of the proposed metric by validating its CA performance predictions with experimental results.

Contents

Declaration	ii
Approval Sheet	iii
Acknowledgements	iv
Abstract	vi
Nomenclature	ix
1 Introduction	1
1.1 WMNs : Architecture and Challenges	1
1.2 Research Problem Outline	3
1.2.1 Problem Definition 1	3
1.2.2 Problem Definition 2	4
1.2.3 Problem Definition 3	4
1.3 Thesis Organization	4
2 Interference in WMNs	6
2.1 Categorizing Interference in WMNs	6
2.2 Interference Models	6
2.3 Selection of Interference Model	8
2.4 Representing Interference in WMNs	8
3 Spatial Co-location of Radios & Radio Co-location Interference	9
3.1 Two RCI Scenarios	9
3.1.1 Case 1 : Trivial Two Node Wireless Network	9
3.1.2 Case 2 : Three WMN Architectures	10
3.2 Experimental Validation	11
3.2.1 Network Design	11
3.2.2 Simulation Results	11
3.3 Impact of RCI on Network Performance	12
4 Proposed MMCG Algorithms	14
4.1 Introduction	14
4.2 Related Research Work	14
4.3 Features of The MMCG Algorithms	16
4.4 Why Two MMCG Approaches?	17
4.4.1 Application Scenarios	17

4.5	The Algorithms : Design and Description	17
4.5.1	The Classical MMCG Algorithm	17
4.5.2	The Enhanced MMCG Algorithm	20
4.6	C-MMCG vs E-MMCG : An Illustration	20
5	Performance Evaluation of the MMCG Algorithms	22
5.1	Measuring Impact of Interference	22
5.2	Application to CA Algorithms	23
5.3	Simulation Setup for Performance Evaluation of CAs	24
5.3.1	Simulation Environment	24
5.3.2	Simulation Design Parameters	24
5.3.3	Data Traffic Characteristics	25
5.3.4	Simulation Terminology, Scenarios and Statistics	26
5.4	Results and Analysis	28
5.4.1	Test Case Class 1	28
5.4.2	Test Case Class 2	29
5.4.3	Test Case Class 3	31
5.5	Summary	34
6	Radio Co-location Aware Channel Assignments	36
6.1	Related Research Work	36
6.2	Features of Proposed RCA CAs	37
6.3	RCA Optimized Independent Set (OIS) CA	38
6.3.1	RCA OIS-CA Algorithm	39
6.3.2	Radio Co-location Optimization	40
6.4	Elevated Interference Zone Mitigation (EIZM) CA	42
6.4.1	RCA EIZM-CA Algorithm	43
6.5	Time Complexities Of Proposed Algorithms	45
7	Performance Evaluation of Radio Co-location Aware Channel Assignments	46
7.1	Simulation Setup	46
7.1.1	Simulation Parameters	46
7.1.2	Data Traffic Characteristics	47
7.1.3	Test Scenarios	48
7.2	Results and Analysis	49
7.2.1	Throughput	49
7.2.2	Packet Loss Ratio	50
7.2.3	Mean Delay	52
7.3	Summary	53
8	Total Interference Degree : A Reliable Metric ?	54
8.1	Inadequacy of TID Estimates : An Example	54
8.2	Correlation Between TID and CA Performance	55
8.2.1	Enlarged CA Sample Set	55
8.2.2	Performance of New CAs	56

8.3	Comprehensive Evaluation of TID Prediction Accuracy	56
8.4	Summary	58
9	Characterization and Estimation of Interference in Wireless Networks	59
9.1	Introduction and Related Research Work	59
9.2	A Fresh Characterization of Interference	60
9.3	Interference Estimation & CA Performance Prediction	60
9.3.1	A Statistical Interference Estimation Approach	61
9.4	Simulations, Results and Analysis	64
9.4.1	Simulation Parameters	64
9.4.2	Traffic Characteristics and Test Scenarios	64
9.4.3	Selection of CA Schemes	65
9.4.4	Results and Analysis	65
9.5	Summary	68
10	Conclusions and Future Work	69
10.1	Conclusions	69
10.2	Future Work	69
	References	71

Chapter 1

Introduction

Wireless Mesh Networks (WMNs) have emerged as a promising technology, with a potential for widespread application in contemporary wireless networks. They have the potential to substitute, and thereby reduce the dependence on the wired infrastructure. In the foreseeable future, WMNs may be extensively deployed due to consistently increasing low-cost availability of the commodity IEEE 802.11 off-the-shelf hardware, smooth deployment with ease of scalability, effortless reconfigurability and increased network coverage [1][2]. The surge in their presence will be equally attributed to the tremendous increase in data communication rates that are being guaranteed by the IEEE 802.11 and IEEE 802.16 standards. WMNs also offer enhanced reliability when compared to their wired counterparts because of the inherent redundancy in the underlying mesh topology. WMN technology, given its practical and commercial appeal, can adequately cater to the needs of a variety of network applications. These networks range from institutional and social wireless LANs, last-mile broadband Internet access, to disaster networks. Prominent wireless technologies that stand to benefit from WMN deployments, other than the IEEE 802.11 WLANs, are the IEEE 802.16 Wireless Metropolitan Area Networks (WMANs) and the next generation cellular mobile systems, including LTE-Advanced [3]. WMNs are also poised to form the backbone of the next-generation of integrated wireless networks, that aim to converge a plethora of technologies such as 3G/4G mobile networks, WLANs etc. onto a single communication delivery platform [4].

1.1 WMNs : Architecture and Challenges

The mesh topology framework in a WMN facilitates multiple-hop transmissions to relay the data traffic seamlessly between source-destination pairs that are often beyond the transmission range of each other [5]. Thus each node in the *Wireless Mesh Backbone* acts as a host and as a router, forwarding packets onto the next hop. A WMN deployment can provide both, a self-contained IEEE 802.11 WLAN with no connectivity to foreign networks, as well as an unrestricted access to outside networks, through a Gateway. Several Gateways may be required if the WMN has to establish communication links with external networks. A simplistic WMN architecture is constituted of numerous mesh-routers which relay/route the data traffic via multiple-hop transmissions, and leverage the twin WMN features of being fully wireless and having a mesh topology. The mesh-clients are the ultimate end-user devices that are serviced by mesh-routers. The mesh-routers constitute the communication backbone of the WMN. Gateways exhibit operational duality by interfacing the WMN with outside networks, besides functioning as any other mesh-router within the WMN.

IEEE 802.11 [6] protocol standards serve as a popular link layer protocol for WMN deployment. A trivial single-gateway WMN is illustrated in Figure 1.1, with mesh-routers and mesh-clients, which is the WMN model we adhere to in this thesis. We consider the availability of multiple radios specifically for inter mesh-router communication, and do not deal with the mesh backbone to mesh-client communication issues. Hereafter, mesh-routers are referred to as nodes.

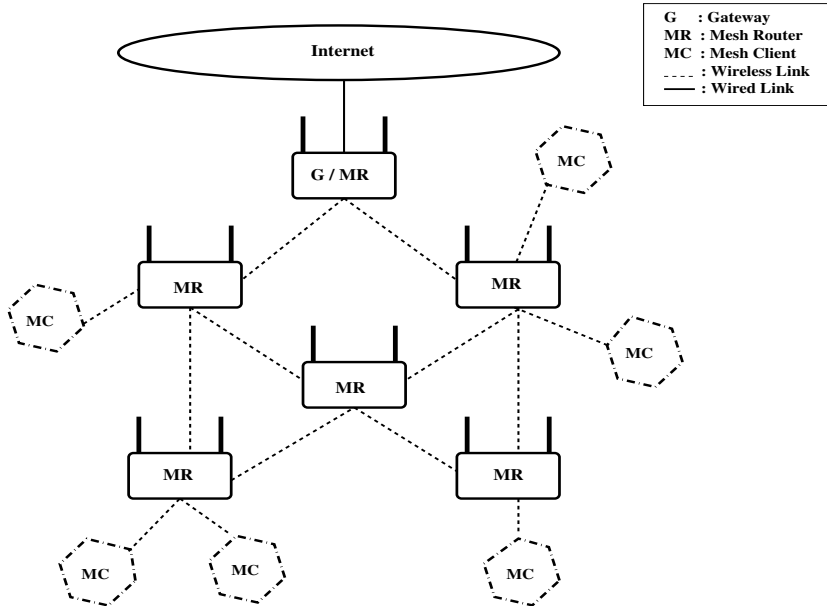


Figure 1.1: A Simplistic WMN Architecture

Initial deployments of WMNs comprised of a trivial single-radio single-channel architecture, in which all nodes were equipped with a single radio and assigned the same channel. Subsequent performance analysis of such wireless network architectures revealed that there was substantial degradation in the network performance metrics, as the size of the WMN is scaled up [7]. Single-channel deployments also adversely affect the end-to-end throughput and network capacity in IEEE 802.11 WMNs [8]. A slightly enhanced architecture is that of the single-radio multi-channel WMNs. But their performance in active deployments has been sub-par, due to the problems of disconnectivity in the WMN topology and the delays in channel switching. In a multi-channel network, assigning different channels to single-radio nodes leads to disruption of wireless connectivity between nodes, even though they lie within the transmission range of each other. Also, dynamically switching to the most suited channel based on the network performance indices, causes a delay of the order of milliseconds [9]. This switching delay is comparable to transmission delays and requires a near-perfect time synchronization between the nodes, so that they are on the same channel when they need to communicate [4].

The most efficient and pervasive WMN architecture is the multi-radio multi-channel conflict (MRMC) framework. Availability of non-overlapping channels under the IEEE 802.11 and IEEE 802.16 standards, and cheap off-the-shelf wireless network interface cards, have propelled the deployment of MRMC WMNs. The IEEE 802.11b/g/n standard utilizes the unlicensed 2.4 GHz frequency band and provides 3 orthogonal channels centered at 25 MHz frequency spacing while the IEEE 802.11a/ac standard operates in the *unlicensed national information infrastructure* band (U-NII

band) that ranges from 5.15 GHz to 5.85 GHz [10]. The assured number of orthogonal channels range from 12 to 24, depending upon the channel bandwidth *i.e.*, 20 or 40 MHz, and the country/region in context. Local laws and policies may restrict access to some frequencies of the 5 GHz band and may also mandate the use of specific communication technologies in the restricted spectrum. For example, in the USA, devices operating in the 5 GHz spectrum are permitted to use only a part of the spectrum, and are required to employ *transmit power control* and *dynamic frequency selection* techniques. The presence of multiple radios on each node coupled with the availability of multiple channels, facilitates concurrent signal transmissions and receptions on the WMN nodes. Thus MRMC WMNs register an enhanced network capacity and an improved spectrum efficiency [9][11]. However, the technological enhancements in WMN deployments have incidentally led to an undesired increase in the interference that impedes the radio communication in such wireless networks.

1.2 Research Problem Outline

Numerous research studies have attempted to address and resolve interference related issues in WMNs. The phenomena of *Radio co-location Interference* or RCI *i.e.*, interference caused and experienced by spatially co-located radios or SCRs, that are operating on identical frequencies, is a crucial aspect of the multifaceted interference problem. But it has been largely unaddressed and finds very little mention in the current WMN research literature. We choose to focus primarily on this issue, and strive to adequately address and mitigate the adverse effects of RCI in a WMN. The first step towards mitigation of the detrimental affects of any interference bottleneck, is its correct identification and representation in the conflict graph. Thus, my thesis accomplishes this goal by an accurate and wholesome representation of all possible RCI scenarios of a WMN in its *conflict graph*. An important objective of this thesis is to propose a fresh characterization of the interference endemic in wireless networks which is not simply based on the source or the cause of interference but represents its inherent characteristics. The third goal of this thesis is to mitigate the impact of interference in WMNs with a special emphasis on RCI alleviation. This objective is achieved by suggesting two CA schemes which are *Radio Co-location Aware* or RCA CAs *i.e.*, they consider RCI as an impeding factor while assigning channels to the radios in a WMN. Finally, this thesis questions the use of *total interference degree* TID estimates as a reliable theoretical measure of CA performance. It addresses the absence of alternate metrics in research literature, which can be employed as well founded theoretical benchmarks for comparison and prediction of CA performance by proposing a *statistical* interference estimation and CA predication scheme. *Interference mitigation in WMNs* is the umbrella research problem, within which this thesis addresses three subproblems elucidated below.

1.2.1 Problem Definition 1

Interference mitigation in WMNs through radio co-location aware conflict graphs

Multi-radio multi-channel conflict graphs or *MMCGs* are frequently used to accurately represent the interference present in a WMN and measure its intensity or degree of impact on the WMN. Thus, a generic approach to create an MMCG for any arbitrary WMN is of utmost importance. The need for a comprehensive procedure to generate an MMCG $G_c = (V_c, E_c)$ for a given input

WMN graph $G = (V, E)$, which is independent of the factors such as the *WMN topology*, the *choice of interference model*, the *channel allocation* scheme etc., is often felt by researchers attempting to solve CA, routing or maximum-throughput problems in a WMN.

To the best of my knowledge, a lucid, all-encompassing and explicitly proposed algorithm for MMCG creation, especially one which factors in the effects of SCRs, is lacking in the current research literature. The novel concept of RCI and the alleviation of its adverse impact on the performance of a WMN, through adequate and accurate representation in the creation of its MMCG, is what distinguishes my study from the plethora of approaches suggested before.

1.2.2 Problem Definition 2

Radio co-location aware channel assignments for interference mitigation in WMNs

Let $G = (V, E)$ represent an arbitrary MRMC WMN comprising of n nodes, where V denotes the set of all nodes in the WMN and E denotes the set of wireless links between nodes which lie within each other's transmission range. Each node i is equipped with a random number of identical radios R_i , and is assigned a list of channels C_i . The number of available channels is greater than the maximum number of radios installed on any node in the WMN. For the WMN described above, we propose *RCA* CA schemes, which allocate channels to every node i in the WMN *i.e.*, $C_i = CA_{RCA}(G)$, so as to efficiently mitigate the detrimental impact of RCI.

1.2.3 Problem Definition 3

Reliable prediction of channel assignment performance in WMNs

Let $G = (V, E)$ represent an arbitrary MRMC WMN comprising of n nodes, where V denotes the set of all nodes and E denotes the set of wireless links in the WMN. Each node i is equipped with a random number of identical radios R_i , and is assigned a list of channels Ch_i from the set of available channels Ch . A reliable theoretical interference estimate needs to be devised to predict with high confidence, the efficient CA schemes that ought to be selected for G from the available set of CA schemes C .

Within the scope of this problem, two more topics are discussed. First, the thesis proposes a fresh characterization of interference, attributing three dimensions, namely, *statistical*, *spatial* and *temporal*, to the interference prevalent in wireless networks. Second, it demonstrates that TID estimates are not suitable to predict the performance of a CA implemented in a given WMN.

1.3 Thesis Organization

In Chapter 2, we touch upon the important interference related themes such as categorization and representation of wireless interference and the *interference models*. Chapter 3 introduces the concept of RCI supplemented with two crucial RCI scenarios, and a *proof of concept* experiment in support of the theoretical arguments. In Chapter 4, we propose two generic multi-radio multi-channel conflict graph generation algorithms, *viz.*, a conventional approach and a novel radio co-location aware approach. Chapter 5 deals with the performance evaluation of the proposed MMCG algorithms. It comprises of simulation methodologies, data traffic characteristics and analysis of recorded results. In Chapter 6, we propose two novel radio co-location aware channel assignment

(RCA CA) approaches. Chapter 7 deals with the performance evaluation of the proposed RCA CAs. In Chapter 8, we discuss the reliability of total interference degree as a theoretical estimate of prevalent interference. In Chapter 9, a new characterization of interference is presented and a statistical interference estimation metric is proposed. Finally, Chapter 9 summarizes the conclusions and outlines the future course of research work. The notable research literature relevant to each topic is included in the chapter presenting it. A summary of analysis of results is also presented at the end of each chapter.

Chapter 2

Interference in WMNs

With the advent of MRMC deployments, the spectral complexity of the WMNs intensified. This led to a substantial rise in the interference endemic in WMNs, identification and mitigation of which continues to be the focus of researchers.

2.1 Categorizing Interference in WMNs

Interference in a WMN can be broadly classified into the following three categories [12].

1. **External** : Interference caused by external wireless devices *i.e.*, un-intentional interferers. It is uncontrolled as external wireless devices may communicate over a common frequency spectrum but are beyond the supervision of the MAC protocol employed in the WMN. Examples are Microwave ovens, Bluetooth devices, and other WMNs or WLANs operating in the same frequency band.
2. **Internal** : Interference originating from within the WMN due to the broadcast nature of wireless communication. A transmission is generally isotropic and causes undesired interference at some of the neighboring nodes of the node for which it is intended. Network topology, channel allocation, and routing schemes have an immense impact on the intensity of internal interference.
3. **Multipath Fading** : It causes inter-symbol interference which occurs when the signals emanated from a particular source take multiple paths to arrive at the destination. The signals differ in time or phase at the destination and interfere with each other.

In this thesis, we focus only on the internal or controlled interference, as it is the primary disruptive component of interference that leads to poor network performance in MRMC WMNs.

2.2 Interference Models

The next step would entail determining the conflicting wireless links in the WMN. This is a very complex problem due to the wireless nature of the network. Hence, researchers employ an accurate network interference model which is suitable for the WMN. The parameters of the model are used to ascertain the interfering or conflicting links. Selection of an appropriate model is crucial in representing complex wireless interference characteristics in a simple mathematical fashion. It is also

pivotal in studying the impact on network performance and behavior, due to the adverse effects of interference. The popular approaches taken to model the interference prevalent in wireless networks are elucidated below [13][14].

1. **The Physical or the Additive Interference Model** : It is the closest representation of the actual physical interference experienced by radios, but is complex to formulate. It takes additive interference into account and considers a fixed *signal to interference plus noise ratio* (SINR) threshold for successful data reception. Since it closely resembles a real-world interference scenario, it is a non-binary interference model. Thus a received signal may be attenuated due to interference, but as long as its strength exceeds the SINR threshold value, it is considered to be a successful transmission.
2. **The Capture Threshold Model** : It is a simplified version of the Physical model which makes use of three threshold values instead of one. Further, the interference modeling is carried out separately for every interfering signal.
3. **The Protocol Model** : In this model, a transmission is successful if it does not experience any interference from other concurrent transmissions in its proximity. Every radio has a transmission and an interference range, where the latter is generally greater than the former. The interference range is usually 2-3 times the transmission range in actual deployments. The protocol model states that a signal transmission from radio R_1 to radio R_2 is deemed successful if R_2 falls within the transmission range of R_1 , but not in the interference range of any other radio which may be active and transmitting concurrently. Consider a graph $G = (V, E)$ which represents a WMN. Here V denotes the set of all nodes in the WMN and E denotes the set of wireless links between node pairs. Further, consider three consecutive nodes of the WMN *viz.*, x_s , x_d and l_s , which lie on the positive X -axis at a distance of x_s , x_d and l_s from the origin, respectively. The protocol model deems a packet transmission on link x (x_s to x_d) successful, if and only if $\forall l \in E - \{x\}$, we have

$$|l_s - x_d| \geq (1 + \Delta) |x_s - x_d| \quad \text{and} \quad (2.1)$$

$$|x_s - x_d| \leq R_c \quad (2.2)$$

Where:

- $(x_s, 0)$ is the source of link x .
 - $(x_d, 0)$ is the destination of link x .
 - $(l_s, 0)$ is the source of other link l whose destination is $(x_d, 0)$.
 - Δ is a positive parameter.
 - R_c stands for the effective range of communication.
4. **The Interference Range Model** : The model mandates the spatial separation between a receiver and an arbitrary interferer to be greater than a fixed quantity *i.e.*, the interference range, for successful transmission. It can be considered to be a simplification of the Protocol model.

2.3 Selection of Interference Model

The Protocol Model is a simplified representation of physical interference which we use in this thesis for three reasons. It is a simple yet felicitous mathematical representation of the actual wireless interference. It permits a binary interference modeling, *i.e.*, a successful transmission is one which is not attenuated by any interfering signal active in its transmission range. Finally, there is no fixed interference range by which two communicating nodes need to be separated. Instead, the model gives us the flexibility of fixing the interference range which is proportional to the distance between a communicating node pair.

2.4 Representing Interference in WMNs

Having successfully identified the interfering wireless links in a WMN, we need to graphically represent their interference relationships. This representation is done by a special graph, called the *Conflict Graph*. We now state a few concepts and definitions. Let $G = (V, E)$ represent an arbitrary WMN.

1. **Potential Interference Link** : Let $i \in V, j \in V$, such that $(i, j) \in E$, then $\forall (m, n) \in E$, where the transmitting range of the radio at node m or n , extends upto, or beyond node i or j , are called the potential interference links of link (i, j) . They are also termed as conflicting links or contention edges.
2. **Potential Interference Number**: Let $i \in V, j \in V$, then the potential interference number of link $(i, j) \in E$, is the total number of links in E which are the potential interference links of (i, j) . It is also called as the *Interference Degree*.
3. **Total Interference Degree (TID)** : It is an approximate estimate of the adverse impact of the interference endemic in a WMN. It is arrived at by halving the sum of the *potential interference numbers* of all the links in the graph.
4. **Conflict Graph (CG)** : $G_c = (V_c, E_c)$ is generated from graph $G = (V, E)$ where
 - $V_c = E$ or $V_c = \{ (i, j) \in E \mid (i, j) \text{ is a wireless communication link } \}$
 - $\{ ((i, j), (m, n)) \in E_c \mid (m, n) \text{ is a potential interference or conflict link of } (i, j) \text{ in } G \}$.

Thus the edges in graph G become the vertices in G_c . There exists an edge between two vertices $x_c \in V_c$ and $y_c \in V_c$, where $x_c = (i, j) \in E$ and $y_c = (m, n) \in E$, iff the corresponding links in edge set E of graph G *i.e.*, (i, j) and (m, n) are conflicting links. In other words, the wireless communication links in the WMN become the vertices in the conflict graph, and any two of these vertices share an edge iff the corresponding wireless links in the WMN interfere with each other.

Chapter 3

Spatial Co-location of Radios & Radio Co-location Interference

An important aspect which most of the existing MMCG creation techniques fail to acknowledge, is the effect of spatial co-location of radios on wireless links, emanating from a node equipped with multiple radios. Such a node certainly stands to benefit if each one of its radios is assigned a different RF channel and can concurrently communicate with adjacent nodes, substantially raising the capacity of the node and the entire network. The throughput at a node and by virtue of aggregation, the capacity of the entire network, can be tremendously accentuated if the RF channels being assigned are non-interfering or orthogonal. However, if two or more SCRs are operating on the same RF channel (or overlapping channels), the multi-radio deployment is rendered ineffective and its advantages are negated. It is also adversely impacted by the additional radio co-location interference generated due to the close proximity of these SCRs. We restrict the study of RCI to SCRs operating on the same channel, which is consistent with the binary interference model that we have adopted. In this chapter, we investigate the impact of spatial co-location of radios on the overall interference dynamics in a WMN. We elucidate two RCI scenarios to support the theoretical proposition, and then experimentally validate the suggested argument.

3.1 Two RCI Scenarios

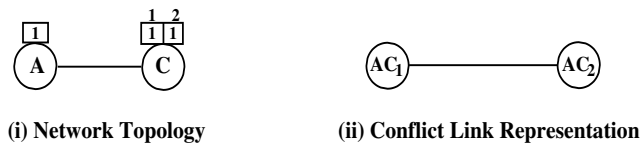


Figure 3.1: Impact of spatially co-located radios

3.1.1 Case 1 : Trivial Two Node Wireless Network

Consider a trivial two node wireless network illustrated in Figure 3.1. Node A is equipped with one IEEE 802.11g radio while node C is equipped with two identical IEEE 802.11g radios *i.e.*, a pair of identical SCRs. Nodes A and C lie within each others transmission range and thus share a wireless communication link in the WMN.

Since the wireless communication link between the nodes A and C is a RF transmission, by virtue of RF wave propagation, any transmission from node A will reach both radio C_1 and radio C_2 alike, as they are co-located at C . Similarly, both radio C_1 and radio C_2 are independently capable of a simultaneous transmission to the radio on node A . In the above scenario, links AC_1 and AC_2 are interfering links and ought to have an edge in the corresponding MMCG to represent their mutual conflict.

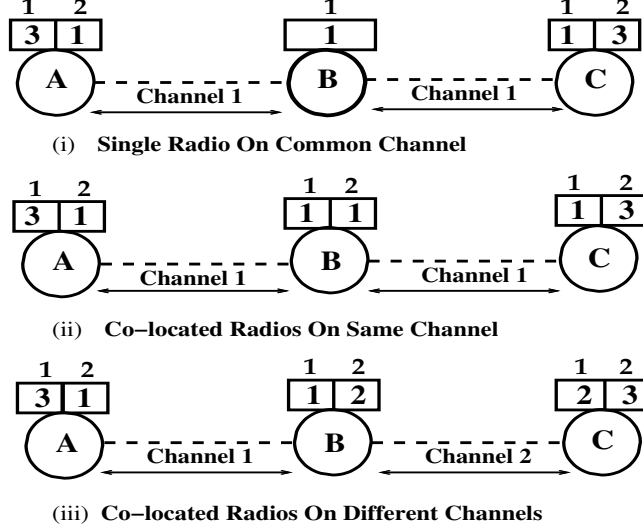


Figure 3.2: Scenarios of radio co-location

3.1.2 Case 2 : Three WMN Architectures

Consider the three flavors of a WMN layout illustrated in the three scenarios of Figure 3.2. The nodes are equipped with one or more IEEE 802.11g radios, which are operating on the depicted radio frequencies. One of the three orthogonal channels 1, 2, & 3, as per the 802.11g specifications, are allocated to the radios. In Figure 3.2 (i), the extreme nodes A and C are equipped with a pair of SCRs, while the node at the center B , has a single radio. In Figure 3.2 (ii), all the three nodes are equipped with a pair of SCRs. Both the scenarios employ common-channel communication, which is evident from the radio-channel allocations. There is, however, a fundamental difference between the two scenarios with respect to node B . Figure 3.2 (i) emulates a *Single-Radio* architecture, rejecting any possibility of RCI. In contrast, Figure 3.2 (ii) has dual radios at node B , both are assigned the same channel, and thus B becomes the epicenter of RCI. The wireless links AB and BC in the depicted WMN layout are the potential conflicting links. Let us focus on node B and reiterate the argument presented in **Case 1** above. For the layout in Figure 3.2 (i), only the radio-links A_2B_1 & C_1B_1 are conflicting links. But for the layout in Figure 3.2 (ii), the total interference degree escalates substantially as there are six conflicting radio-link pairs, viz. A_2B_1 & A_2B_2 , A_2B_1 & B_1C_1 , A_2B_1 & B_2C_1 , A_2B_2 & B_1C_1 , B_2C_1 & B_1C_1 and A_2B_2 & B_2C_1 . In the WMN layout in Figure 3.2 (iii) the wireless links AB and BC are represented by the radio-links A_2B_1 and B_2C_1 . They have been assigned channels 1 and 2, respectively, and therefore are non-conflicting links. This scenario fully utilizes the inherent multi-radio multi-channel architecture, leading to an interference free deployment.

Drawing from the stated theoretical arguments we contend that in the considered trivial WMN layout, the *Single Radio Common Channel* (SRCC) operation in Figure 3.2 (i) will perform better, even if marginally, than the *Multi Radio Common Channel* (MRCC) operation in Figure 3.2 (ii). Further, the *Multi Radio Different Channel* or *MRDC* deployment in Figure 3.2 (iii) will significantly outperform the other two configurations.

3.2 Experimental Validation

To corroborate my argument with actual experimental data, simulations of the three network layouts illustrated in Figure 3.2 were performed in ns-3 [15].

3.2.1 Network Design

The inbuilt ns-3 TCP BulkSendApplication is employed to establish two TCP connections between node pairs A & B and B & C , for the scenarios (i), (ii), and (iii) of Figure 3.2. We install a TCP *BulkSendApplication* source at the nodes A & C . Both the TCP sinks are installed at node B , as it is the node common to all the conflicting links, and hence the focal point of maximum interference offered to the data communication. Every source sends a *10 MB* data file to its corresponding sink. We observe the *Network Aggregate Throughput* for each of the three scenarios, which serves as a fair metric to gauge the adverse impact of interference in the WMN layout. Simulation parameters are listed in Table 3.1.

Table 3.1: Co-location Experiment Simulation Parameters

Parameter	Value
Transmitted File Size	10 MB
Maximum 802.11 Phy Datarate	9 Mbps
RTS/CTS	Enabled
TCP Packet Size	1024 Bytes
Fragmentation Threshold	2200 Bytes
Inter-node Separation	250 mts
Propagation Loss Model	Range Propagation

3.2.2 Simulation Results

I register the throughput of only the onward flow, *i.e.*, the *Source - Sink* flow, for both TCP connections of each deployment, and illustrate the *Average Aggregate Network Throughput* recorded for the three scenarios, in Table 3.2.

Table 3.2: Co-location Experiment Simulation Results

Parameter	SRCC	MRCC	MRDC
Average Aggregate Network Throughput (Mbps)	3.19	3.01	5.87

The *SRCC* deployment performs slightly better than the *MRCC* deployment. This result vindicates the theoretical contention, that the surge in interference due to SCRs operating on a common

channel, degrades the network performance substantially. Here, the difference in the *Average Network Aggregate Throughput* of the two deployments is less than 10%, which is not remarkable. However, we should consider the fact that in medium to large MRMC WMNs, the presence of SCRs which have been assigned the same channel is in moderate to large numbers. This increase in SCRs will exacerbate the adverse effects of RCI on the network performance. The *Multi-Radio Different-Channel* or the *MRDC* deployment offers an *Aggregate Network Throughput*, that is almost twice that of a trivial *SRCC* deployment. This is in conformity with my theoretical supposition as well. We can safely conclude, that the results of this investigation substantiate the proposed theoretical concept of RCI *i.e.*, the *interference caused by SCRs* which have been assigned a common-channel.

3.3 Impact of RCI on Network Performance

The severity of RCI in a wireless network depends upon the number of SCRs that have been assigned an identical channel. The two factors which decide the impact of RCI are, the number of available orthogonal channels offered by the wireless technology and the number of radios that a node in a wireless network is equipped with. We now elaborate on these factors.

- **Number of orthogonal channels :** Availability of orthogonal channels depends upon the wireless communication technology being used. For example, IEEE 802.11g radios operating in the 2.4 GHz spectrum have only 3 orthogonal channels at their disposal. Therefore, RCI has a significant impact on network performance as we have demonstrated. However, 12 to 24 non-overlapping channels are available to the IEEE 802.11n/ac radios operating in the 5 GHz spectrum. This will ensure that SCRs are seldom assigned identical channels, and the impact of RCI is minimal.
- **Number of radios per node :** The number of radios installed on a wireless node depends upon the size, cost and most importantly, the power or energy consumption of a radio. These three factors limit the number of radios that can be installed on a node.

There are two primary reasons why addressing the impact of RCI on WMNs is of great significance. First, IEEE 802.11g/n radios operating in the 2.4 GHz band are being used in Wi-Fi networks across the globe, especially in the developing countries. This thesis will demonstrate the severity of impact that RCI has on medium to large WMNs employing the 802.11g standard through extensive simulations. Thus, RCI alleviation measures and techniques will immensely benefit these WMN/WLAN deployments. Second, in the IEEE 802.11n/ac networks operating in 5 GHz spectrum, currently the number of available orthogonal channels far exceeds the number of radios installed on a node. But in the foreseeable future, this relationship may change and even be reversed. My argument is based on the developments made in the field of radio hardware in the last decade. Significant inroads have been made in the development of carbon nanotube based nanoradios [16], first proposed by the well known physicist Alex Zettl. A communication architecture for nanoradios has been proposed in [17] which provides an operational framework for the carbon nanotube based nanoradios. Further, in [18] authors discuss the significance of current pioneering research in the field of nanoradios, and describe the role nanonetworks are poised to play in revolutionizing the modern communication networks. With the advent of nanoradio technology, it will not be unrealistic to imagine a single wireless device equipped with dozens of nanoradios. In addition, the challenge of energy constraints

in radio communication will be met through innovations in the field of micro-power and nano-power systems [19]. Taking these developments into consideration, it is possible that in future the number of radios present on a node in a WMN will be quite comparable to the number of available orthogonal channels. Thus, the impact of RCI in such wireless networks will be highly detrimental.

It is thus imperative that we take cognizance of the RCI phenomena, and address its adverse impact on the performance of a WMN. The first step of this exercise would be to account for and appropriately represent the co-location interference scenarios in the interference model of a WMN. But the representation of RCI is lacking in the MMCG creation method suggested in [20], and all other research works aimed at minimization of interference in WMNs. The underlying reason is that while creating the MMCG, the fact that multiple radios installed on the same node are spatially co-located is overlooked. A result of this oversight is that a few interference scenarios escape notice during the MMCG creation and the estimate is seldom a true reflection of the actual interference present in the network. This thesis adopts a fundamental approach towards RCI mitigation, which is through creation of radio co-location aware MMCGs. Since no prior research work focuses on the impact of RCI on WMNs and its mitigation, it makes this thesis relevant and indispensable.

Chapter 4

Proposed MMCG Algorithms

4.1 Introduction

Interference substantially degrades the wireless network performance. It leads to low end-to-end throughputs, high packet loss and high transmission delays. Multi-hop transmissions in WMNs are adversely impacted by the co-channel interference, which deteriorates network capacity and destabilizes fairness in link utilization [8]. Addressing the issue of internal co-channel interference in a WMN is of foremost importance in WMN deployments. While designing network topology, efforts are made to limit the impact of interference by optimal node placement. An MRMC architecture is better suited to be interference resilient as compared to simpler architectures. Significant research work has been carried out towards alleviating the inimical impact of interference on WMN performance. For example, several MAC protocols for WMNs have been proposed [21], nodes equipped with high-power directional antennas have been deployed [1], etc. But these solutions limit the scalability and span of WMNs, and are not practically viable. Thus, the most crucial design choices to ensure interference minimization in WMNs without limiting their scalability are : channel assignment (CA) to radios, link scheduling and routing. Numerous CA schemes [10], and a multitude of routing algorithms [22] have been contributed in the effort to mitigate and restrain the impact of interference in WMNs.

4.2 Related Research Work

Conflict graphs serve as the primary indispensable tool for addressing various design and performance issues in WMNs. They are extensively used for modeling and estimating the interference degree in wireless and cellular networks [20]. However, a basic conflict graph (CG) is only suited to a wireless network in which each node is equipped with a single radio. In order to model the interference in an MRMC WMN, the concept of *CG* needs to be extended to an enhanced version called the *multi-radio multi-channel conflict graph* or an *MMCG*. Several research endeavors [23, 10, 4, 24, 25, 26, 27, 28, 29, 20, 30, 31], directed at finding an efficient CA scheme for an MRMC WMN have made use of the concept of MMCG to model the interference in their network scenario. In [4], the authors merely suggest that the conflict graph was generated by ensuring that the *interference-to-communication* ratio is set to 2, with no further insight into the algorithmic aspects of this crucial step. In contrast, the literature in [23] defines two approaches to generate conflict graphs. The first definition is centered on the *traffic flow interference*, employing the protocol model and assuming unidirectional traffic flows. The second approach takes into account the

link interference based on the extended protocol model. However, it is evident that neither of the proposed techniques is inherently generic in its outlook. The former assumes a unidirectional traffic flow and mandates the application of the protocol model as the underlying interference model, while the latter necessitates the use of the extended protocol model, restricting both their approaches to specific WMN architectures. Likewise, authors in [10] define a conflict graph to be an undirected graph under the protocol model.

Authors in [24] provide a high level definition of CG, with an assurance that the concept is applicable to any interference model. However, they do not explicitly propose any algorithm. Further, they opine that a CG does not change with the assignment of channels to vertices. This is not a true characteristic of the MMCG of a WMN, as it often changes when different CA schemes are deployed in the WMN. Assignment of different channels to a link, under different CAs, alters the set of its conflict links, thereby generating a different MMCG for each CA. Thus the authors' contention that a CG for a WMN will not change, does not hold true, at least in the context of an MRMC deployment.

Authors in [25] discuss a single-channel CG and its multi-channel peer (MMCG) for the protocol model, without suggesting a methodical approach to generate either. In addition, they map a link to a unidirectional flow, and a bidirectional traffic is represented by two links. This underscores the fact that researchers tend to perceive the interference dynamics which are a common feature of all WMNs, in a personalized way specific to their WMN model, rather than adopting a broadly applicable view. In [26], the authors lay a special emphasis on *weighted* conflict graphs for the protocol model. For non-interfering or non-overlapping channels, they recommend that a CG should be generated for each individual channel, and the CG for the WMN will be the union of all single channel CGs. Thus they take a single-channel view of an MRMC WMN, applied to multiple channels, and the final MMCG is an aggregate of the unique individual single channel CGs. The approach is intuitive and simple, but for a medium to large scale WMN where each node is equipped with multiple identical NICs, and which leverages the availability of a high number of non-interfering channels, this fragmented view of a WMN to arrive at an MMCG will cause substantial implementation overhead.

The human perception of interference scenarios plays a significant role in the generation of a conflict graph. For example, the representation of WMN conflict relationships in the MMCG proposed in [28] is quite different than the one suggested in [29]. The work in [28] aims to create a multi-dimensional CG by making use of a radio-link-channel tuple, while authors in [29] create a link-layer flow contention graph which is essentially a simple CG, that is based upon the number of channels allocated and the channel assignment to interfaces. Based on the review, we opine that the most generic and widely applicable of all MMCG creation procedures is suggested by *Ramachandran et. al.* [20]. The authors extend the conflict graph concept to model a multi-radio WMN, and generate a *multi-radio conflict graph* or an *MCG*. They describe the MCG generation approach explaining the use of an improvised vertex coloring algorithm to color the MCG, which ensures that each radio in the network is assigned a single channel. Yet, a lucid algorithm to generate the MCG is not proposed in the study. Any correlation between the MCG creation approach and the underlying interference model is not presented either. This leaves room for ambiguity in determining the dependence of the MCG creation technique upon the interference model being employed. Most importantly, the suggested approach and the corresponding illustration does not address the interference caused and experienced by SCRs operating on identical frequencies, and

thus fails to represent the RCI scenarios in its interference estimate. From the literature review presented above, we can conclude that the underlying fundamental concepts of a conflict link and a basic conflict graph, have been rightly employed by researchers in their work. However, the creation of an MMCG in the research studies often depends upon one or more of the following factors.

1. The Interference Model being used, which is the *protocol model* in most studies.
2. The WMN Topology
3. Representation of Traffic Flows *i.e.*, unidirectional or bidirectional
4. Perception of the interference scenarios

Further, we have not come across any research study related to MMCG generation that adequately addresses or even highlights, the detrimental effect of multiple SCRs installed at a WMN node, which have been assigned the same channel to communicate on. To remedy the lack of a generic algorithm, we now propose two comprehensive polynomial time algorithms to create a multi-radio multi-channel conflict graph or an *MMCG*. The first algorithm we propose, does not take into account the effect of spatial co-location of multiple radios on a node. It follows a conventional approach, variations of which have been employed in various research endeavors, customized to suit the model being implemented. However, a versatile algorithm which is independent of the aforementioned constraints has not been formally proposed, a void this thesis aims to bridge. I christen it *The Classical MMCG* algorithm, or *C-MMCG*. The second algorithm effectively factors the RCI into its interference modeling logic. It paints a more comprehensive and wholesome picture of the interference scenario in the given WMN, and is thus a notable improvement over *C-MMCG*. We name it *The Enhanced MMCG* algorithm, or *E-MMCG* for ease of reference.

4.3 Features of The MMCG Algorithms

The algorithms are designed with the vision of creating a widely applicable and versatile method of generating MMCGs. We ensure their structural and functional independence from the commonly encountered constraints listed below.

1. ***The Choice of Interference Model***: As stated earlier, this thesis employs the protocol interference model to determine the interfering links. This however, is not binding upon the algorithms, and any other interference model can be chosen instead. The algorithms allow the underlying interference model to define a conflicting link. Thus the choice of the interference model is not an implementation constraint.
2. ***WMN Topology***: The algorithms are topology independent and applicable to all WMN deployments. The graphical representation, however, must be a connected graph. This condition is reasonable, necessary and not an impediment, as having an isolated node with no wireless connectivity to any other node in the WMN is wasteful.
3. ***Number of Radios and Channels*** : The algorithms are also applicable to both single channel and multi-channel WMN deployments *i.e.*, they can create MMCGs for the same WMN topology for both, a common CA and a varying/multiple CA.

4. **The Channel Assignment or CA Scheme** : The algorithms can generate an initial *multi-radio conflict graph*, whose edges denote potentially interfering links when every radio is assigned the same channel. They can as easily generate a *multi-radio multi-channel conflict graph* or an MMCG, which depicts the actual state of interference in a WMN deployment in where a CA scheme is implemented. The output MMCGs will certainly differ if the CA scheme implemented in the network changes.
5. **Interpretations of Interference Scenarios**: The algorithms, especially the one which takes RCI into account, consider every possible interference scenario in the WMN. Thus, they avoid the variations associated with the human interpretations of interference scenarios.

4.4 Why Two MMCG Approaches?

The purpose to produce and discuss both the algorithms is two-fold.

1. To algorithmically demonstrate the difference between the two approaches.
2. Further, to determine two different channel assignments for a WMN, employing the two conflict graph approaches, C-MMCG and E-MMCG, and compare the network performance of the two CAs.

4.4.1 Application Scenarios

The two broad scenarios in a WMN where the proposed MMCG algorithms find great utility are elucidated below.

1. *Prior to CA* : Before the CA exercise is carried out in a WMN, usually all the radios are assigned a default channel. The MMCG resulting from this default channel configuration represents a maximal prevalent interference scenario and thus serves as an ideal input to a CA algorithm.
2. *After CA* : After the radios have been assigned appropriate channels in accordance with the applied CA scheme, the proposed MMCG algorithms may be used to generate the TID estimate for the WMN. This desirable feature facilitates a theoretical assessment of the efficacy of the CA approach employed.

4.5 The Algorithms : Design and Description

Now we propose the two algorithms along with their functional description.

4.5.1 The Classical MMCG Algorithm

The *C-MMCG* algorithm adopts a conventional approach to model the interference endemic in WMNs. Its stepwise procedure is described in Algorithm 1. Steps 1 to 10 split each node in the original WMN topology graph $G = (V, E)$, into the number of radios it is equipped with, and generate an intermediate graph $G' = (V', E')$, where V' represents the set of total number of wireless radios in the WMN and E is edge set of links between radio pairs.

Algorithm 1 C-MMCG : Radio Co-location Not Considered

Input: $G = (V, E)$, $R_i(i \in V)$, $N_i(i \in V) = \{ j | (j \in V) \ \&\& \ (i \neq j) \ \&\& \ ((i, j) \in E) \}$

Initially : $V' \leftarrow \emptyset$, $E' \leftarrow \emptyset$, $V_c \leftarrow \emptyset$, $E_c \leftarrow \emptyset$

Notations : $G \leftarrow$ WMN Graph, $R_i \leftarrow$ Radio-Set, $N_i \leftarrow$ Neighbour Set

Output: $G_c = (V_c, E_c)$

```
1: for  $i \in V$  do
2:    $V' \leftarrow V' + R_i$ 
3:   for  $j \in N_i$  do
4:     for  $x \in R_i$  do
5:       for  $y \in R_j$  do
6:          $E' \leftarrow E' + (x, y)$ 
7:       end for
8:     end for
9:   end for
10: end for{Get the intermediate graph  $G' = (V', E')$ }
11: for  $(i, j) \in E'$  where  $i \in V', j \in V'$  do
12:    $V_c \leftarrow V_c + (i, j)$ 
13: end for{Create the Vertex Set  $V_c$  of the CG  $G_c$ }
14: for  $v \in V_c, u \in V_c, v \neq u$  do
15:   Use an Interference Model to determine if  $u$  &  $v$  are Potentially Interfering Links
16:   if True then
17:     if ( $Channel(u) == Channel(v)$ ) then
18:        $E_c \leftarrow E_c + (u, v)$  {Create the Edge Set  $E_c$  of the CG  $G_c$ }
19:     end if
20:   end if
21: end for{Output C-MMCG  $G_c = (V_c, E_c)$ }
```

While G reflects a node centric view of the WMN, G' reflects the view of the WMN at the granularity of individual radios. Step 2 splits the radio set of each node in G to individual radio-nodes in G' . Steps 3 to 10, process the neighbor set of a node in G to create edges in E' , for each individual radio in the radio-set of the node in context. The intermediate graph G' becomes the input for the final MMCG creation step. In steps 11 to 13, the vertex set V_c of the MMCG is populated by adding elements of the edge-set E' . Further, in steps 14 to 21, the vertices in V_c are processed pairwise, and a corresponding edge is added to the MMCG edge-set E_c , *iff* the vertex pair being currently processed is conflicting, and both the vertices have been assigned the same channel. The function $Channel()$ fetches the channel assigned to a particular vertex of G_c . As described earlier, the channel returned by the function would be the default channel if the algorithm is being applied to a WMN prior to the CA exercise. Else, $Channel()$ would fetch the channel that has been assigned by the CA scheme employed in the WMN. The underlying interference model determines whether a vertex pair is conflicting. We have employed the *Protocol Interference Model*, but as stated earlier, any other interference model may be used as well. Algorithm 1 finally outputs the *C-MMCG*, G_c . The algorithmic time complexity is $O(n^2)$, as each of the three functional steps *viz.*, creating the intermediate graph G' , generating the vertices of C-MMCG G_c , and finally adding the edge set to C-MMCG G_c , have an $O(n^2)$ computational complexity, where n is the number of nodes in the WMN.

Algorithm 2 E-MMCG : Radio Co-location Considered

Input: $G = (V, E)$, $R_i (i \in V)$, $N_i (i \in V) = \{ j | (j \in V) \ \&\& \ (i \neq j) \ \&\& \ ((i, j) \in E) \}$

Initially : $V' \leftarrow \emptyset$, $E' \leftarrow \emptyset$, $V_c \leftarrow \emptyset$, $E_c \leftarrow \emptyset$

Notations : $G \leftarrow$ WMN Graph, $R_i \leftarrow$ Radio-Set, $N_i \leftarrow$ Neighbour Set

Output: $G_c = (V_c, E_c)$

```
1: for  $i \in V$  do
2:    $V' \leftarrow V' + R_i$ 
3:   for  $j \in N_i$  do
4:     for  $x \in R_i$  do
5:       for  $y \in R_j$  do
6:          $E' \leftarrow E' + (x, y)$ 
7:       end for
8:     end for
9:   end for
10: end for {Get the intermediate graph  $G' = (V', E')$ }
11: for  $(i, j) \in E'$  where  $i \in V', j \in V'$  do
12:    $V_c \leftarrow V_c + (i, j)$ 
13: end for {Create the Vertex Set  $V_c$  of the CG  $G_c$ }
14: for  $v \in V_c, u \in V_c, v \neq u$  do
15:   Use an Interference Model to determine if  $u \&v$  are Potentially Interfering Links
16:   if True then
17:     if ( $Channel(u) == Channel(v)$ ) then
18:        $E_c \leftarrow E_c + (u, v)$  {Create the Edge Set  $E_c$  of the CG  $G_c$ }
19:     end if
20:   end if
21: end for
22: for  $v \in V_c, u \in V_c, v \neq u ; v = (a, b), u = (c, d) ;$ 
    $a, b, c, d \in V'$  do
23:   for  $i \in V$  do
24:     if [ $\{(a \in R_i || b \in R_i) \ \&\& \ (c \in R_i || d \in R_i)\} \ \&\& \$  (Both elements of  $R_i$  on same channel)]
       then
25:        $E_c \leftarrow E_c + (u, v)$ 
26:     end if
27:   end for
28: end for {Output E-MMCG  $G_c = (V_c, E_c)$ }
```

4.5.2 The Enhanced MMCG Algorithm

The *E-MMCG* considers all possible interference scenarios that exist in a WMN, including the RCI. The stepwise procedure to generate an E-MMCG for a WMN is described in Algorithm 2. In addition to the *C-MMCG* logic, Algorithm 2 also captures interference due to spatial co-location of radios in the WMN. In steps 22 to 28, the algorithm adds an edge between two vertices of the E-MMCG, **iff**

1. The corresponding pair of wireless links in the WMN originate or terminate at the same node and,
2. The links have been assigned the same channel.

The RCI accounting steps will apply to both common and multiple channel deployments in the WMN, preserving its generic nature. E-MMCG thus ensures that the interference scenarios discussed earlier, which are not being addressed in the existing research literature are accounted for. Further, the injection of the RCI into the overall interference dynamics is duly represented by addition of necessary and sufficient links in the E-MMCG. The links added to the E-MMCG to account for the RCI, are characteristic of the E-MMCG algorithm, and are generated from its steps 22 to 28. These conflicting links may or may not be determined by the employed interference model, but they will definitely not escape notice of the E-MMCG algorithm. The time complexity of the algorithm, similar to its conventional counterpart C-MMCG is $O(n^2)$.

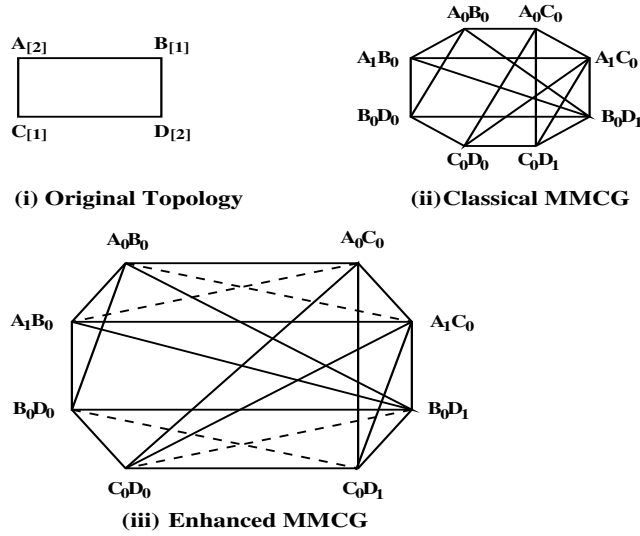


Figure 4.1: An illustration of Classical and Enhanced MMCGs for a given Topology

4.6 C-MMCG vs E-MMCG : An Illustration

Let us pictorially demonstrate the output MMCGs for the two flavors proposed above, through Figure 4.1. Figure 4.1 (i) depicts the original WMN topology comprising of four nodes, A , B , C and D , where the nodes are assigned 2, 1, 1, and 2 number of radios, respectively. Each radio is operating on the default channel, so the two methods will generate the initial, maximal-conflict MMCG for the WMN. The graphical representations of C-MMCG and E-MMCG, for the given

WMN layout, are exhibited in cases (ii) and (iii) of Figure 4.1, respectively. Upon observation, it is evident that E-MMCG has all the conflicting links present in C-MMCG, and in addition contains four more interfering links, *viz.* $A_0B_0 - A_1C_0$, $A_1B_0 - A_0C_0$, $B_0D_0 - C_0D_1$ and $C_0D_0 - B_0D_1$. These four conflicting links are the result of RCI, which is caused by the wireless transmissions from radios spatially co-located at nodes A and D .

The number of these additional conflict links caused by RCI increases drastically with the size of the WMN, which we demonstrate in the next section. The ability of E-MMCG algorithm to capture and represent the interference scenarios spawned by RCI is the first step towards alleviating the adverse impact of RCI.

Chapter 5

Performance Evaluation of the MMCG Algorithms

Having proposed the two MMCG algorithms, it is imperative we prove their relevance to real-world WMN deployments. We take a three pronged approach in this regard.

5.1 Measuring Impact of Interference

We employ the MMCG algorithms to measure the TID in a WMN, and compare the results of the two flavors. we consider a square *Grid Layout* for the WMNs, of size $5n \times 5n$ where $n = \{1, 2, \dots, 10\}$. Thus the size of WMNs varies from 5×5 nodes to 50×50 nodes, where all the nodes are equipped with 2 identical radios, and all radios are on a *common channel*. This configuration represents a *maximal interference* scenario, and is ideal for analysis. We apply both the MMCG algorithms to each of these grid topologies. The results illustrated in Figure 5.1 underscore the fact that the E-MMCG algorithm accounts for all the *potential interfering links* or *interference scenarios* present in a WMN, and hence registers substantially high values of *TID*.

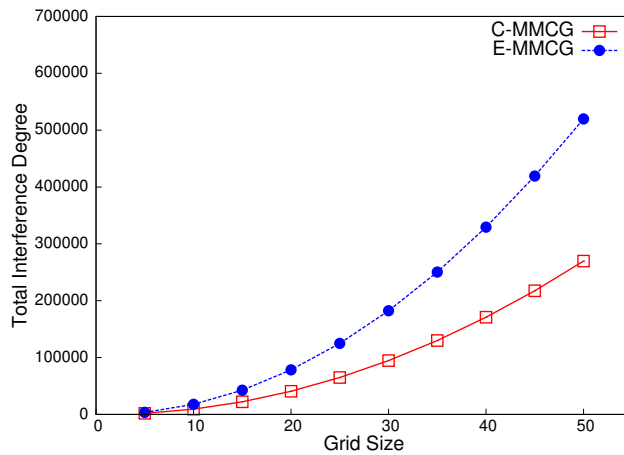


Figure 5.1: TID Comparison of *C-MMCG* vs *E-MMCG*

In contrast, the C-MMCG algorithm suffers from a limited potency to probe a WMN for *potential interfering links* as it does not factor in the presence of SCRs operating on a common channel. This is reflected by its poor accounting of *Interference Degree* values as compared to its enhanced counterpart, the E-MMCG. Further, as the size of WMN grows, the difference in the *TID* of the two MMCG approaches becomes increasingly prominent. This implies that there is a tremendous upsurge

in the RCI as the size and complexity of the WMN increases. This finding further consolidates the proposition the thesis puts forward in Chapter 3, that the adverse impact of RCI gets more pronounced in medium to large WMNs.

5.2 Application to CA Algorithms

Since *Conflict Graphs* serve as the input to *Channel Assignment* algorithms, the next logical step is to apply the MMCG algorithms to two graph-theoretic solutions of the CA problem. In [20] authors propose a *Breadth First Search* approach or BFS-CA, which is a centralized dynamic algorithm that employs the services of a *channel assignment server* or CAS. Initially, the radios in the WMN are assigned a default channel which experiences the least interference from intentional or un-intentional interferers in close proximity, based on a channel-ranking technique. The CAS computes the average distance of each vertex in the multi-radio conflict graph (MCG) from the gateway. Thereafter, the algorithm performs a breadth-first scan of the MCG, starting from the vertices closest to the gateway, and assigns a channel to every vertex that it encounters. To every vertex, CAS tries to assign a channel which is orthogonal to the channels assigned to its neighboring nodes. Else, it selects a channel randomly from the set of available channels and allots it to the current vertex. A *Maximal Independent Set* channel assignment scheme or MaIS-CA is proposed in [31]. It is a greedy heuristic scheme, which determines the maximal independent set of vertices in a conflict graph, assigns them an identical channel and then removes them from the conflict graph. This process is iterated, until all the vertices have been assigned a channel.

I opine that MaIS-CA is algorithmically superior to BFS-CA as its CA approach distributes the channels among the radios in a more balanced fashion, and also assures a higher degree of connectivity in the WMN graph. For a theoretical validation of the stated notion, we implement these two CA algorithms in Grid WMNs. Both C-MMCG and E-MMCG versions serve as the input to CA schemes, and the *TID* for each CA scheme is determined. The nodes are equipped with 2 identical radios each, and utilize the 3 non-overlapping channels guaranteed by IEEE 802.11g specifications. For a smooth discourse hereon, we adopt the following nomenclature to differentiate between the CAs.

- *C-MMCG based CAs* : BFS-CA₁ and MaIS-CA₁.
- *E-MMCG based CAs* : BFS-CA₂ and MaIS-CA₂.

The procedure followed is described below :

- Take WMN grid of size $n \times n$, where $n \in \{3, 5, 10\}$.
- Create two *MMCGs* using the algorithms C-MMCG and E-MMCG.
- Use both flavors of MMCG as input to BFS-CA and MaIS-CA to obtain final CAs, 4 in all.
- Apply C-MMCG on BFS-CA₁ & MaIS-CA₁ and E-MMCG on BFS-CA₂ & MaIS-CA₂, to estimate their respective *TIDs*.

This procedure will furnish the theoretical measure of the impact of interference in each of the final CAs. For consistency, we subject a particular version of a CA only to the corresponding MMCG algorithm, to compute the *TID* estimate. Further, we only compare two CAs generated from the

Table 5.1: A Comparison of TIDs of the MMCG CAs

Grid Size	TID			
	BFS-CA		MaIS-CA	
	C-MMCG	E-MMCG	C-MMCG	E-MMCG
3×3	82	70	16	56
5×5	436	716	142	488
10×10	2098	2470	834	2036

same MMCG approach. Comparing the interference estimate of a C-MMCG CA with an E-MMCG CA is not logical, because the approaches to generate these estimates are not identical.

It can be inferred from Table 5.1, that the BFS-CA of a particular MMCG version registers a higher measure of interference than the corresponding MaIS-CA, *i.e.*, with respect to *TID* of CAs, $BFS-CA_1 > MaIS-CA_1$ and $BFS-CA_2 > MaIS-CA_2$. This result strengthens the argument that MaIS-CA is a better CA scheme than BFS-CA. Further, it offers a theoretical assurance that employing the use of E-MMCG approach does not alter the intrinsic algorithmic disposition of a CA.

5.3 Simulation Setup for Performance Evaluation of CAs

The final step in this research investigation entails that we monitor and analyze the performance of BFS-CA and MaIS-CA, for both versions of the MMCG, through comprehensive simulations.

5.3.1 Simulation Environment

We create an extensive data traffic scenario by considering various single-hop and multi-hop transmission combinations. The objectives are four fold.

1. To compare the performance characteristics of E-MMCG CA against that of the C-MMCG version, for the same CA algorithm.
2. To compare the performance of the two approaches, BFS-CA and MaIS-CA, for both versions of MMCG.
3. To observe the relative difference between the performances of BFS-CA and MaIS-CA, in the two versions of MMCG.
4. To observe the traffic interruptions or abrupt flow terminations, for a CA, in both versions of MMCG.

Through objectives (b) and (c) above, we intend to study the consistency in CA performance *i.e.*, if *X-CA* performs better than *Y-CA* in the C-MMCG model, then we opine that it should outperform *Y-CA* in the E-MMCG model as well. Further, we study the difference between the performances of *X-CA* and *Y-CA* for a relative comparison.

5.3.2 Simulation Design Parameters

I consider a 5×5 grid WMN, which provides some semblance of a large-scale topology. To gauge the impact of interference on the WMN, we choose the *Aggregate Throughput* of the network, as the primary performance metric. The total capacity of a network consistently degrades with the increase in interference, and it is thus a suitable and sufficient metric. We also employ *Packet Loss*

Ratio and *Mean Delay* of the network as metrics for some scenarios. While Packet Loss Ratio gives a measure of data packets lost during communication, the Mean Delay provides the end-to-end latency in packet transmission. Thus both of them are reliable indicators of the disruption caused in data transmission by the prevalent interference.

TCP and UDP are the underlying transport layer protocols being used in the experiments. The inbuilt ns-3 models of *BulkSendApplication* and *UdpClientServer* are utilized for TCP and UDP implementations, respectively. TCP simulations are aimed at estimating the *Aggregate Network Throughput* while the UDP simulations are employed to determine the *Packet Loss Ratio* and the *Mean Delay*. For ease of reference, hereon we denote the three metrics as Throughput_{Net}, PLR and MD, respectively.

The radios installed on all nodes are identical IEEE 802.11g radios, operating in the standard specified 2.4 GHz spectrum that offers up to 14 channels, of which 3 channels are orthogonal. We restrict the number of available channels to these 3 non-interfering channels. We employ the *ERP-OFDM* modulation technique, with a ceiling of 9 Mbps on the maximum *PHY* data-rate. We let the transmission power assume the default value of 16.02 dBm, and set the receiver gain to -10 dBm for better sensitivity. Nodes are placed at a separation of 200 mts, so that the adjacent nodes lie comfortably within each other's transmission range. Use of *Range Propagation Loss Model* in ns-3 facilitates an easy implementation of the *protocol model* for interference modeling. The remaining simulation parameters are listed in the Table 5.2.

Table 5.2: ns-3 Simulation Parameters

Parameter	Value
Grid Size	5 × 5
No. of Radios/Node	2
Range Of Radios	250 mts
Available Orthogonal Channels	3
Maximum 802.11 PHY Datarate	9 Mbps
Maximum Segment Size (TCP)	1 KB
Packet Size (UDP)	1KB
Fragmentation Threshold	2200 Bytes
RTS/CTS(TCP)	Enabled
RTS/CTS(UDP)	Disabled
Routing Protocol Used	OLSR
Loss Model	Range Propagation
Propagation Model	Constant Speed

5.3.3 Data Traffic Characteristics

The most critical step in studying the impact of interference in a WMN is to tailor the right set of traffic flows, which will identify and expose the interference bottlenecks. To simulate a data traffic with suitable characteristics, we consider five types of TCP/UDP traffic flows which include both, single and multi-hop flows. We deploy a combination of these flow-types to characterize the intensity of interference present in a 5 × 5 grid WMN. The 25 nodes in the WMN grid are numbered from 1 to 25, for the sake of representation. The traffic flows are depicted in Figure 5.2, followed by a brief description of each flow. The TCP/UDP client or *source*, can be identified by the dotted tail of the

link representing the TCP/UDP connection, while the arrow-head signifies the TCP/UDP server or the *sink*.

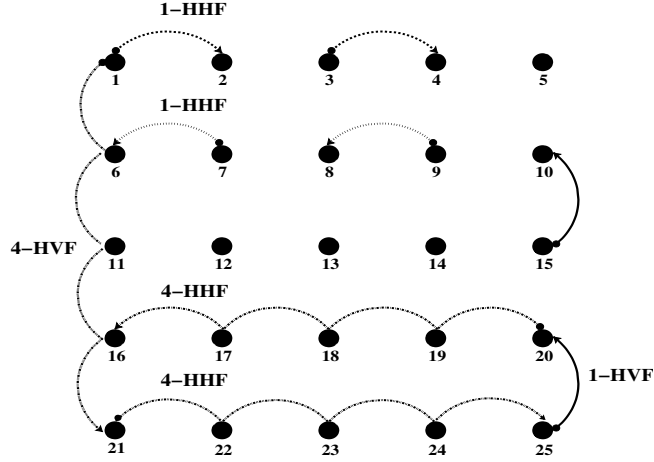


Figure 5.2: Grid Layout

1. *One Hop Horizontal Flow or 1-HHF* : Single Hop TCP connections are established between alternate node pairs in all the rows of the WMN grid depicted in Figure 5.2. For example, in row 1, node-pairs (1 & 2) and (3 & 4) have a one hop TCP connection. TCP source application is installed on the node represented by a smaller number, and the sink application on the node bearing the bigger number in the node-pair.
2. *One Hop Vertical Flow or 1-HVF* : In addition to the 1-hop horizontal flows, one hop TCP vertical flows, between alternate node-pairs in each column in the bottom-up direction, are also generated.
3. *Four Hop Horizontal Flow or 4-HHF* : Since multi-hop transmission is an inherent trait of WMNs, we deploy TCP/UDP connections between the first and last nodes of each row, which are four hops away.
4. *Four Hop Vertical Flow or 4-HVF* : To capture the spatial interference characteristics of the grid in the vertical direction, TCP/UDP connections are established in a top-down fashion *i.e.*, between the first and last nodes of each column, which are four hops away.
5. *Eight Hop Diagonal Flows or 8-HDF* : The diagonally opposite node-pairs (1 & 25) and (21 & 5) have a TCP/UDP connection each, and generate eight-hop TCP/UDP flows. This is the maximum possible hop-length between a source and destination pair, in the given simulation grid.

5.3.4 Simulation Terminology, Scenarios and Statistics

To keep the discourse lucid and coherent, we first define some terms used in the upcoming sections.

1. *Flow* : It refers to the onward TCP/UDP traffic flow from a TCP/UDP source to the TCP/UDP sink.

2. *Abrupt Flow* : In all the TCP connections, we mandate that the source should transmit *10 MB* data to the sink. For a TCP connection to be deemed successful, it is imperative that the sink should receive the *10 MB* data sent by the source in entirety. Else, the TCP connection is considered to have abruptly terminated, and the flow to be an *Abrupt Flow*. Abrupt flows are a measure of the obstructions caused by prevalent interference to the data transmissions in a WMN. This notion is predicated on the fact that routing failures are often caused by high levels of interference in multi-hop wireless networks [32]. Loss of routing information causes packets buffered at intermediate relay nodes to be dropped. Since the routing protocol is singularly responsible for the routing mechanism, a TCP source may never be aware of an alternate route or route re-establishment. Thus, after subsequent failed attempts at re-transmitting the packets, a connection-timeout is invoked at the source and eventually the flow is abruptly terminated.
3. *Abrupt Flow Count* (AFC) : It is the total number of Abrupt Flows encountered in all the simulations of a *Test Case Class*.
4. *Throughput_{Net}* : It refers to the *Network Aggregate Throughput*, which is the aggregate throughput of all the flows in a simulation.
5. *Flow-RX* : A 4-HHF TCP flow in any row *X* of the grid.
6. *Flow Type-Y or FT-Y* : A set of all possible combinations of 4-HHFs taken *Y* at a time, where $Y \in \{1..5\}$. Thus, FT-1 would be a set containing 5C_1 or five 4-HHFs, viz. Flow-R1, Flow-R2, Flow-R3, Flow-R4 and Flow-R5.

I segregate the simulation scenarios into combinations of one-hop flows and multi-hop flows. The underlying motivation is to monitor the behavior of CAs for single-hop flows, and more complex multi-hop flows, separately. The test-cases have been categorized into the following three classes.

1. Test Case Class 1 : Flow Sustenance Testing

In the test-cases belonging to this class, numerous one-hop TCP connections are concurrently active. The motivation here is to highlight the capability of a WMN to establish and sustain multiple TCP connections under the debilitating effects of interference. Thus, these test-cases are focused on the number of abrupt flows encountered *i.e.*, the AFC, rather than the Throughput_{Net} . The test-cases under this class are listed below.

- (a) *Test Case 1* : Only vertical flows *i.e.*, 1-HVFs.
- (b) *Test Case 2* : Only horizontal flows *i.e.*, 1-HHFs.
- (c) *Test Case 3* : All vertical and horizontal flows *i.e.*, 1-HVFs + 1-HHFs.

2. Test Case Class 2 : Flow Injection Testing

Multi-hop transmissions are a primary characteristic of WMNs. Concurrent multi-hop data connections are the perfect instruments for estimating the adverse impact of interference on the network capacity, as they transmit in tandem, triggering and intensifying the intricate interference bottlenecks in a WMN. We start with a single 4-HHF, and then inject one additional 4-HHF in each subsequent test-case. We monitor the network response to injection of fresh four-hop flows in terms of the network capacity, for a variety of 4HHF combinations.

Here we focus only on monitoring the throughput response of the network and not the number of abrupt flow terminations.

The goal here is to record the variation in network performance with the continuous injection of additional four-hop flows, hence it will suffice to do so for flows along the rows of the grid. We consider the five 4-HHF's *i.e.*, Flow-R1...Flow-R5, and create a test-case for each *Flow Type-Y* or *FT-Y*, where $Y \in \{1...5\}$. Thus, we have the following test-cases.

- (a) *Test Case 1* : FT-1 *i.e.*, 5C_1 4-HHF combinations.
- (b) *Test Case 2* : FT-2 *i.e.*, 5C_2 4-HHF combinations.
- (c) *Test Case 3* : FT-3 *i.e.*, 5C_3 4-HHF combinations.
- (d) *Test Case 4* : FT-4 *i.e.*, 5C_4 4-HHF combinations.
- (e) *Test Case 5* : FT-5 *i.e.*, 5C_5 4-HHF combinations.

3. Test Case Class 3 : Load or Stress Testing

A reliable measure of network performance is often gauged under peak load, as it exhibits a network's resilience to bottlenecks that occur only at high traffic demands. We perform four test-cases of increasing data traffic demands. By virtue of the rise in the number of concurrent radio transmissions, there is an increase in the interference complexities of the network. For each of these scenarios, we observe and analyze not only the network capacity, but also the packet loss ratio (PLR) and mean delay (MD). Thus both TCP and UDP simulations are run for each of the the test-cases described below.

- (a) *Test Case 1* : D2 *i.e.*, Concurrent twin diagonal TCP/UDP flows or 8-HDFs.
- (b) *Test Case 2* : H4V4 *i.e.*, Eight Concurrent TCP/UDP flows comprising of adjacent 4-HHF and 4-HVFs, each taken four at a time. A total of four such combinations, for which simulations are run and the average $Throughput_{Net}$ is considered.
- (c) *Test Case 3* : H5V5 *i.e.*, Ten concurrent TCP/UDP flows consisting of all five 4-HHF's and all five 4-HVFs.
- (d) *Test Case 4* : H5V5D2 *i.e.*, Twelve concurrent TCP/UDP flows consisting of all five 4-HHF's, all five 4-HVFs, and both 8-HDFs.

5.4 Results and Analysis

The four CAs *viz.*, BFS-CA₁, BFS-CA₂, MaIS-CA₁ and MaIS-CA₂, are subjected to the test-cases described above. The metrics we monitor and register for subsequent analysis are *Throughput_{Net}*, *AFC*, *PLR* and *MD*. We now present the recorded results, and methodically analyze them in adherence to the four objectives stated in sub-section 6.3.

5.4.1 Test Case Class 1

The metric of relevance here is the *Abrupt Flow Count* or AFC, which for C-MMCG CAs is quite higher than the corresponding E-MMCG CAs. This can be inferred from the graph displayed in Figure 5.3. BFS-CA₂ is able to achieve a 12.7% reduction in abrupt termination of flows over

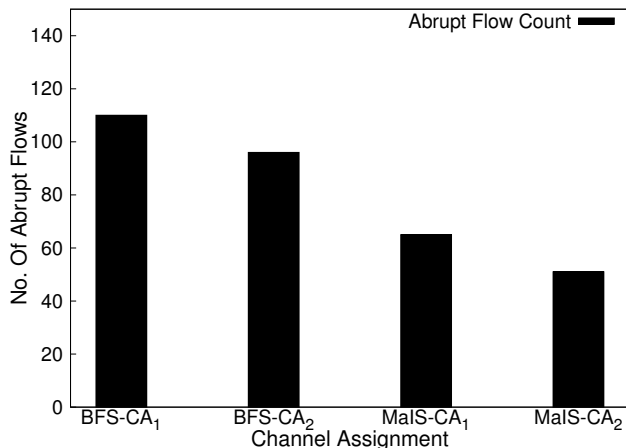


Figure 5.3: Abrupt Flow Count in Test Case Class 1

BFS-CA₁. Likewise, we record a 21.53% drop in AFC for MaIS-CA₂, when compared to MaIS-CA₁. Further, a comparison of the two CA approaches underscores the consistency of MaIS-CA in outperforming BFS-CA, for both the MMCG approaches. MaIS-CA₁ registers 40.9% lesser abrupt flow terminations than BFS-CA₁, and this improvement is more accentuated in MaIS-CA₂ where the frequency of abrupt flows depreciates by 46.8% when compared to BFS-CA₂.

From the perspective of relative performance in terms of Abrupt Flow Count, E-MMCG approach heightens the edge that MaIS-CA has over BFS-CA. This is evident from the *relative decrease* in AFC of 14.4% achieved in the E-MMCG CAs, over their C-MMCG peers. This result is arrived at by the simple expression $(\% \text{ Drop in E-MMCG} - \% \text{ Drop in C-MMCG}) / \% \text{ Drop in C-MMCG}$. Thus, the E-MMCG CAs not only reduce the abrupt terminations of flows when compared to the respective C-MMCG versions, but also enhance the performance of a better CA scheme (MaIS-CA) when compared to a less efficient algorithm (BFS-CA).

Throughput_{Net} is not an ideal metric to compare the CA performances in *Test Case Class 1*, but for consistency the Throughput_{Net} results are presented in Table 5.3. MaIS-CA performs unarguably better than BFS-CA which is in accordance with the TID estimates shown in Table 5.1. In all the test-cases E-MMCG CAs perform slightly better than their C-MMCG peers. The only exception is observed in *Test Case 2 i.e.*, Only 1-HHF, where MaIS-CA₁ > MaIS-CA₂. This reversal is rectified in *Test Case 3 i.e.*, All 1-HHF and 1-HVF, which is a more comprehensive test scenario and a relatively better case for observing Throughput_{Net}.

5.4.2 Test Case Class 2

I now analyze the response of the CA deployments in the WMN in terms of observed Throughput_{Net}, as new four-hop flows are injected in the network. Results of *Test Case Class 2*, which consists of a variety of multi-hop test-cases, are exhibited as a graph in Figure 5.4. The Throughput_{Net} recorded for each of the five test-cases in this class, represented by *FT-Y*, where $Y \in \{1...5\}$, is plotted for the four CA schemes. It is clearly evident that the E-MMCG version of a CA outperforms the C-MMCG version by a significant margin. For a reference, we quote the statistics of FT-5 from Figure 5.4, for all the four CAs. The Throughput_{Net} values of BFS-CA₁, BFS-CA₂, MaIS-CA₁, and MaIS-CA₂, are recorded to be *1.711 Mbps*, *1.88 Mbps*, *2.26 Mbps* and *3.36 Mbps*, respectively. We process the

Table 5.3: Throughput_{Net} in Test Case Class 1

Network Throughput (Mbps)			
BFS-CA		MaIS	
Test Case 1 → 1-HVFs			
<i>BFS-CA₁</i>	<i>BFS-CA₂</i>	<i>MaIS-CA₁</i>	<i>MaIS-CA₂</i>
16.73	18.40	24.31	24.44
Test Case 2 → 1-HHF			
<i>BFS-CA₁</i>	<i>BFS-CA₂</i>	<i>MaIS-CA₁</i>	<i>MaIS-CA₂</i>
19.05	20.41	21.95	19.55
Test Case 3 → 1-HVFs + 1-HHF			
<i>BFS-CA₁</i>	<i>BFS-CA₂</i>	<i>MaIS-CA₁</i>	<i>MaIS-CA₂</i>
24.99	25.36	32.35	34.16

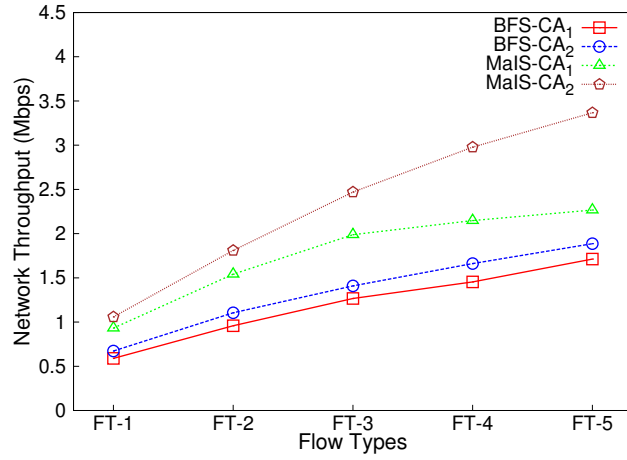


Figure 5.4: Throughput_{Net} in Test Case Class 2

results to determine the change, *i.e.*, increase or decrease, in the observed Throughput_{Net} values of the two variants of the same CA, in Table 5.4. The Throughput_{Net} value of the C-MMCG version of a CA is considered as the base.

Table 5.4: % Change in Throughput_{Net} values of an E-MMCG CA over corresponding C-MMCG CA in Test Case Class 2

CA Strategy	% Change in Throughput _{Net} in FT				
	1	2	3	4	5
BFS	13.9	15.2	11.2	14.3	10.2
MaIS	13.4	17.4	24.2	38.7	48.5

Throughput_{Net} values of BFS-CA₂ are higher than those of BFS-CA₁ for all Flow Types, however always within the modest range of 10% to 15.2%. A more prominent increase in Throughput_{Net} can be noticed in MaIS-CA₂ with respect to MaIS-CA₁. The rise in Throughput_{Net} values ranges from 13.4% in FT-1, to a maximum of 48.5% in FT-5. This increase in Throughput_{Net} of MaIS-CA₂, continues to rise from Flow Type-1 to Flow Type-5, *i.e.*, with the increase in the number of concurrent flows injected in the network. The second objective is to assess how the two CA schemes fare against one another, in both the MMCG models. It can be inferred that MaIS-CA

performs substantially better than BFS-CA, irrespective of the MMCG model. However, it is of great relevance to study the variation of the difference in Throughput_{Net} values recorded for the two CA schemes, in the two MMCG models. Thus, we compute the % difference in Throughput_{Net} values of BFS-CA and MaIS-CA for each MMCG model in Table 5.5. Throughput_{Net} values of BFS-CA are considered as the base, and the % increase or decrease of MaIS-CA over BFS-CA is calculated, for the particular MMCG variant. A % decrease, is preceded by a negative sign.

Table 5.5: % Difference in Throughput_{Net} values of BFS-CA and MaIS-CA for an MMCG approach in Test Case Class 2

MMCG Model	% Difference in Throughput_{Net} in FT				
	1	2	3	4	5
C-MMCG	58.1	60.7	56.8	47.7	32.3
E-MMCG	57.4	63.7	75.3	79.2	78.4
Relative Difference (%)	-1.2	4.9	32.5	66	142

In the C-MMCG deployment, MaIS-CA₁ records a significant increase over BFS-CA₁ that falls in the range of 32.3% to 60.7%. In the E-MMCG deployment, MaIS-CA₂ surpasses its C-MMCG variant, registering tremendous increase over BFS-CA₂ Throughput_{Net} is in the range of 57.4% to 79.2%. Further, we calculate the *relative difference* of the increase in Throughput_{Net} that MaIS-CA shows over BFS-CA, between the two MMCG models, as a % with C-MMCG as the base. The relative difference is slightly negative at (-1.2%) for FT-1, but this result is not unsettling for two simple reasons. First, that FT-1 is a minimalistic test scenario with just one 4-HHF active at a time, and second being the diminished magnitude of this relative decrease. Besides, the % relative increase rises immensely from FT-2 through FT-5, to reach a high of 142% at FT-5, which is the most comprehensive interference scenario.

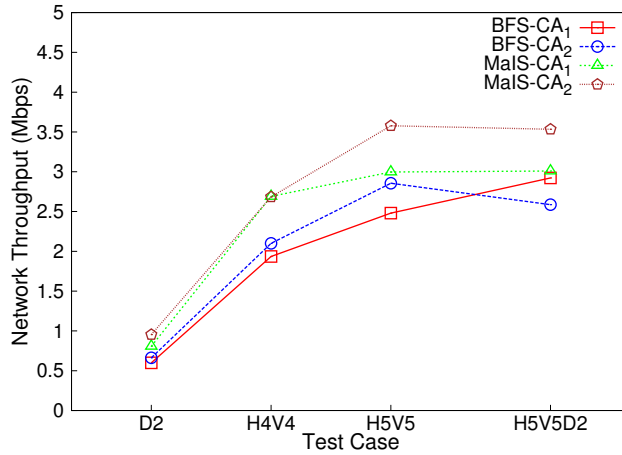


Figure 5.5: Throughput_{Net} in Test Case Class 3

5.4.3 Test Case Class 3

This class of test-cases is aimed at measuring the network performance in terms of Throughput_{Net} ,

PLR and MD, under heavy network data traffic. The test-cases of this class are complex as they involve a high number of concurrent multi-hop TCP/UDP connections, causing almost every interference scenario to affect the data transmission. The Throughput_{Net} results of the *stress testing* exercise are presented for analysis in the graphs depicted in Figure 5.5. The overall performance of E-MMCG CAs continues to be better than their corresponding C-MMCG peers, but we can observe a few deviations from the trend. In test-case H4V4, MaIS-CA₁ registers a higher Throughput_{Net} than MaIS-CA₂ although by an insignificant margin of 0.24%. Further, in the peak load scenario H5V5D2, the Throughput_{Net} of BFS-CA₁ is higher than that of BFS-CA₂ by 11.4%, which can be noticed in Table 5.6. The two instances in which a C-MMCG CA performs equal to or better than the corresponding E-MMCG CA do not raise any doubts about the efficacy of the E-MMCG model, but instead highlight the temporal and spatial characteristics of the endemic interference. Even a reasonably good CA scheme may register a sub-par performance for a particular traffic scenario. In all the remaining test-cases, the E-MMCG CAs outperform their C-MMCG counterparts, registering noticeable increase in Throughput_{Net} that falls within the range of 8.4% to 19.3%.

Table 5.6: % Change in Throughput_{Net} values of an E-MMCG CA over corresponding C-MMCG CA in Test Case Class 3

CA Strategy	% Change in Throughput_{Net} in Test Case			
	D2	H4V4	H5V5	H5V5D2
BFS	10.4	8.4	15.1	-11.4
MaIS	18.2	-0.2	19.3	17.4

Let us now examine how the two CA schemes fare against one another, in the two MMCG models. In Table 5.7, the % difference in Throughput_{Net} values of BFS-CA and MaIS-CA for each MMCG model is computed. MaIS-CA proves to be better than BFS-CA, regardless of the MMCG model employed. Secondly, the % difference between the E-MMCG CAs is more pronounced in all scenarios except for the test-case H4V4, where it is 27.8% while it is 39% for the C-MMCG model. This reversal is the outcome of the fact that both versions of MaIS-CA *viz.* MaIS-CA₁ and MaIS-CA₂, demonstrate similar Throughput_{Net} characteristics in H4V4, while BFS-CA₂ registers a higher value than BFS-CA₁ as expected. Thus, the % relative difference of the increase in Throughput_{Net} that MaIS-CA shows over BFS-CA, between the two MMCG models, is positive for all test scenarios except for test-case H4V4.

Table 5.7: % Difference in Throughput_{Net} values of BFS-CA and MaIS-CA for an MMCG approach in Test Case Class 3

MMCG Model	% Difference in Throughput_{Net} in Test Case			
	D2	H4V4	H5V5	H5V5D2
C-MMCG	34.6	39.0	20.8	3.0
E-MMCG	44.0	27.8	25.3	36.6
Relative Difference (%)	27.2	-28.7	21.6	1124.1

Moving on to the observed PLR values, let us examine the graph in Figure 5.6 and the corresponding processed results in Table 5.8. In all test-cases, the E-MMCG CAs suffer from a much lesser PLR than the respective C-MMCG CAs, thereby implying a reduced impact of interference

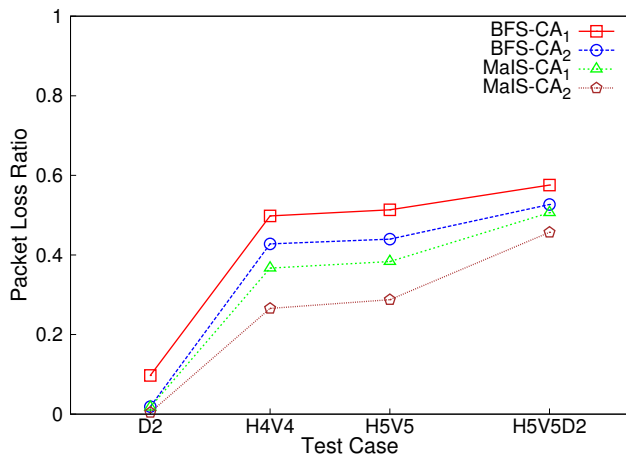


Figure 5.6: Packet Loss Ratio in Test Case Class 3

on the data transmissions. Further, in accordance with the earlier result trends, PLR results also highlight that MaIS-CA₂ registers a greater reduction in PLR over MaIS-CA₁ than BFS-CA₂ does over BFS-CA₁. The % relative difference of decrease in PLR values that MaIS-CA shows over BFS-CA, between the two MMCG models, is positive for all values except D2 where it is -5.9% . For the remaining test-cases the relative difference is positive, always above 10% and as high as 43%. Thus we can infer that the E-MMCG model accentuates the decrease in PLR registered by MaIS-CA over BFS-CA, as compared to the C-MMCG model where this decrease is less prominent.

Table 5.8: % Reduction in Packet Loss Ratio of an E-MMCG CA over corresponding C-MMCG CA in Test Case Class 3

CA Strategy	% Reduction in PLR in Test Case			
	D2	H4V4	H5V5	H5V5D2
BFS	80.7	14.1	14.3	8.4
MaIS	75.5	27.5	25.0	9.7

Table 5.9: % Difference in Packet Loss Ratio between BFS-CA and MaIS-CA for an MMCG approach in Test Case Class 3

MMCG Model	% Difference in PLR in Test Case			
	D2	H4V4	H5V5	H5V5D2
C-MMCG	82.0	26.3	25.3	12.0
E-MMCG	77.1	37.8	34.6	13.2
Relative Difference (%)	-5.9	43.7	36.7	10.1

The final metric of interest here is the mean delay (MD), the recorded results for which are depicted in the graph in Figure 5.7. Deviating from the pattern of other metrics, MaIS-CA does not command a clear advantage over BFS-CA with respect to MD. In fact, the observed values for the two CAs fluctuate and can not be compared, which is easily discernible from Figure 5.7. For most test-scenarios BFS-CA₂ registers the minimum MD values performing better than even MaIS-CA₂. Therefore, we restrict the analysis to reduction in MD that an E-MMCG CA registers over its corresponding C-MMCG CA. The processed results are presented in Table 5.10. Both MaIS-CA₂ and BFS-CA₂ boast of a reduced MD than MaIS-CA₁ and BFS-CA₁, respectively. The difference

between the two versions of BFS-CA is more pronounced which is a shift from the result patterns observed earlier. Nevertheless, the E-MMCG CAs succeed in reducing packet transmission latency in the WMN grid as compared to their conventional counterparts.

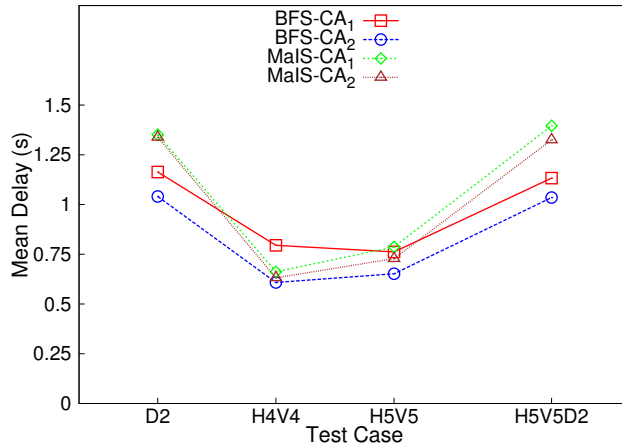


Figure 5.7: Mean Delay in Test Case Class 3

Table 5.10: % Reduction in Mean Delay of an E-MMCG CA over corresponding C-MMCG CA in Test Case Class 3

CA Strategy	% Reduction in MD in Test Case			
	D2	H4V4	H5V5	H5V5D2
BFS	10.5	23.5	14.4	8.6
MaIS	1.0	4.5	7.4	5.0

Through these experiments we have successfully demonstrated that the same CA scheme exhibits better performance when it receives an E-MMCG as input, as compared to a C-MMCG as input. The E-MMCG ensures that a lesser number of SCRs are assigned identical channels by the CA scheme, which in turn leads to a decrease in RCI in the network. Further, the proposed MMCG algorithms enable a CA scheme to reduce the link conflicts and minimize the impact of interference, but do not make any assumptions or place any restrictions on the functioning of the CA schemes. Thus, the MMCG algorithms do not alter the algorithmic disposition of a CA scheme.

5.5 Summary

I begin by drawing the most fundamental conclusion that RCI has an adverse effect on the performance of WMNs. The *Enhanced MMCG* model accounts for and adequately represents the RCI caused by spatially co-located radios. It is thus better equipped and algorithmically more tuned to alleviate the adverse impact of interference, than its conventional counterpart the *Classical MMCG* model. The efficacy of a CA scheme in successfully mitigating the RCI depends on the extent of its knowledge of the conflict links that originate from RCI. The conventional MMCG generation techniques including the proposed C-MMCG approach, fail to account for and represent the RCI induced link conflicts in the MMCG model. The E-MMCG of a WMN remedies this problem by making the CA scheme aware of the prevalent RCI scenarios, thereby enabling it to assign channels

to radios in a manner that restrains the RCI.

I can safely conclude that the CA deployments under the E-MMCG model invariably perform better than their peers under the C-MMCG model, for all the network performance indices. The improvement noticed in MaIS-CA is substantial as compared to BFS-CA where a less pronounced improvement was observed. Therefore, though the E-MMCG model augments the performance metrics of a CA, the underlying CA strategy also plays a determining role in this enhancement. This inference is a positive feature of the E-MMCG model that it does not alter or modify the inherent behavior or algorithmic nature of a CA scheme.

Chapter 6

Radio Co-location Aware Channel Assignments

The benefits of increased throughput, enhanced connectivity and reduced latency promised by a multi-radio multi-channel (MRMC) WMN are predicated upon the feature of reduced interference that is not a characteristic of the network itself, but instead, of the channel assignment (CA) scheme. Minimizing the interference in a WMN is thus a fundamental system design and operational objective and the most crucial aspect of achieving this goal is an optimum and feasible CA to the radios in the WMN. A prudent CA will reign in the interference and its detrimental effects and in turn enhance the capacity of the mesh network and improve overall network performance.

6.1 Related Research Work

In Chapter 3, we have discussed the phenomena of *radio co-location interference* (RCI) and its detrimental impact on the performance of a WMN, a problem domain that has so far remained largely unaddressed. RCI is caused and experienced by spatially co-located radios at a node, that have been allocated identical channels to communicate on. We proposed an *Enhanced Multi-Radio Multi-Channel Conflict Graph* (E-MMCG) model, which enables a CA algorithm to mitigate the adverse impact of RCI and substantially enhances the performance of the deployed CA. The E-MMCG model takes into account the interference scenarios spawned and experienced by the spatially co-located radios (SCRs) at a node in the WMN, and adequately represents them in its conflict graph (CG). The E-MMCG model accomplishes this by adding an edge between two vertices of the conflict graph if and only if, the respective wireless links in the WMN emanate from or terminate at the same node, and have been assigned an identical channel. The E-MMCG thus generated is a comprehensive representation of all possible conflict links in a WMN, including the RCI scenarios, and serves as an ideal input to CA schemes.

The CA problem is an NP-Hard problem [33], and substantial research effort has been focused towards finding efficient CAs for WMNs, yet to the best of my knowledge, no proposed CA scheme incorporates RCI alleviation as a design objective. The CA approaches can be broadly classified into three categories, *viz.* static, dynamic and hybrid. A static scheme mandates a fixed radio-channel mapping throughout the session for which the network is operational. Dynamic CA features updating of the CA continuously, based on the analysis of network metrics, for better efficiency and throughput. They can be both centralized and distributed. Hybrid CAs employ characteristics of both static and dynamic CA schemes, efficiently assigning a fixed CA to some radio interfaces and a dynamic CA to others. Several CA schemes have been proposed in earlier research studies [34], of

which we mention a few. A centralized Breadth First Traversal (BFT) approach BFS-CA, has been suggested in [20] where channels are assigned to nodes, after performing a BFT with the Gateway node as the reference. A static maximum clique based algorithm is discussed in [25]. In [31] authors proposed MaIS-CA, a Maximum Independent Set (MIS) based high performance CA, where MIS of the *conflict graph* (CG) is determined iteratively, and channels are assigned to the nodes of the MIS in each step. A centralized static CA scheme is proposed in [30], where nodes of the CG are assigned channels so that the Total Interference Degree (TID) decreases, resulting in an efficient CA. TID is a theoretical estimate which gives a measure of the intensity of the interference prevalent in a WMN. It is the sum of the individual *conflict numbers* of all links, where conflict number of a link represents the total number of potential link conflicts experienced by that particular link in a WMN.

However, the absence of RCI mitigation as a crucial design consideration is bound to hamper the efficiency of a CA, as it does nothing to restrain the RCI. Thus, it is imperative that CA algorithms be *Radio Co-location Aware* or RCA *i.e.*, consider RCI as an impeding factor while assigning channels to the radios in a WMN. In this chapter, we propose two RCA CA algorithms. The schemes are static, as the primary bottlenecks in dynamic and hybrid CAs are the channel switching delays, and the need of a mechanism for co-ordination between nodes to ensure that they are on the same channel when they intend to communicate [9].

6.2 Features of Proposed RCA CAs

I now present the two RCA CA algorithms. The proposed algorithms benefit from the following design considerations.

Enhanced Conflict Graph Model

RCA CA algorithms ought to employ the use of the E-MMCG model [35] to generate the E-MMCG of a WMN, which usually serves as the input to CA schemes. This broad-based model accounts for the prevalent RCI and adequately represents it in the CG of the WMN.

Efficient Radio Co-location Optimization

This is the signature functionality of the RCA CA algorithms. It ensures that spatially co-located radios are not allocated identical channels to communicate on. In addition, it may also serve as an optimization step by restraining the detrimental effect of interference over network performance.

Spatio-Statistical Interference Alleviation

A static CA, due to its inherent rigidity of radio-channel mapping, can only address the spatio-statistical aspects of the three dimensional interference-mitigation problem, the third dimension being the temporal or dynamic characteristics. A scheme primarily catering to the spatial features of interference will effect a CA in which links on identical or overlapping channels are efficiently interspersed with links operating on respective orthogonal channels. An intelligent spatio-statistical scheme, in addition to spatial prudence, will strive to evenly distribute the available channels among the radios, thereby facilitating an efficient CA with enhanced fairness.

Network Topology Preservation

The apparent trade-off between ensuring connectivity at the cost of increased interference, holds its relevance in reduced propagation delays between end-nodes, and seamless uninterrupted connectivity to the end-user. Further, a CA approach should not alter the original WMN topology to ensure the functional independence of physical spatial design of the WMN from the channel allocation exercise. We opine that the WMN topology ought to be preserved after a CA deployment.

Thus the proposed algorithms are graph theoretic approaches which restrain the RCI by leveraging the twin interference mitigation features, *viz* the E-MMCG model and Radio Co-location Optimization and also incorporate spatial and statistical dimensions of the prevalent interference in their structural design, to fashion efficient high-performance RCA CAs.

Notations common to both the algorithms are, G : The WMN graph, G_c : E-MMCG of the WMN graph, CS : The set of M available channels, Adj_i : The set of nodes adjacent to node i in G , Ch_i : The list of channels allocated to the radios of node i in G ; It may have duplicate elements, which will reflect the impact of RCI at node i . $TID(G)$: The function which computes the *total interference degree* (TID) *i.e.*, the estimate of prevalent interference in a WMN.

6.3 RCA Optimized Independent Set (OIS) CA

This graph-theoretic RCA CA scheme appeals to the statistical aspects of channel assignment. We contend that, given two CA schemes with similar spatial patterns, the one with a more proportionate distribution of available channels among the radios of the WMN will perform better. We will validate this argument with TID estimates, and further through rigorous simulations.

The method of assigning channels to radios based on the Maximal Independent Set or MIS approach finds numerous references in the research literature [36] [31]. However, we contend that the MIS approach is not statistically pragmatic with respect to the channel allocation exercise, and an IS approach stands to fare better. For example, the MaIS scheme elucidated in [31] suggests that in each iteration, an MIS of the updated CG be determined, all vertex elements of the MIS be assigned a common channel and then removed from the CG. By its very definition, an MIS can not add even a single vertex to its element set lest it violate its independence. Further, an MIS may or may not be a *maximum* IS. Yet, we can infer that as the cardinality of the vertex set of the CG decreases in subsequent iterations, the MaIS scheme is disposed to generate MISs with decreasing cardinalities as well. Now, since a channel is assigned to all the vertices in an MIS in each step, the distribution of channels among radios is bound to be uneven. To validate my argument, we employ MaIS algorithm to generate CAs for WMN grids of size $(N \times N)$, where $N \in \{5, \dots, 9\}$. Every node is equipped with two identical radios and there are three orthogonal channels C_1 , C_2 & C_3 , available to be assigned to a radio. C_1 is the default channel on which all radios were initially operating to generate the E-MMCG. We ascertain the statistical evenness of a CA for a WMN grid by determining the ratio of the number of radios operating on each channel denoted by R_{C_1} , R_{C_2} & R_{C_3} , normalized by the smallest value observed for a channel. The results are illustrated in Table 9.1. It can be discerned that there is a skewed distribution of channels among the radios. The number of radios which are allocated C_3 is always at least 50% more than those on C_1 , which is the default channel and is consistently under utilized in the final CA. The difference between R_{C_2} and R_{C_1} is also never below 33%, highlighting a statistically uneven allotment of channels to radios.

Table 6.1: Equitable channel distribution, RCA OIS-CA vs MaIS-CA

Grid Size	Num of Radios	$R_{C1} : R_{C2} : R_{C3}$	
		MaIS	RCA OIS
5×5	50	1.00 : 1.63 : 1.94	1.00 : 1.06 : 1.06
6×6	72	1.00 : 1.33 : 1.66	1.00 : 1.09 : 1.33
7×7	98	1.00 : 1.56 : 1.69	1.00 : 1.00 : 1.16
8×8	128	1.00 : 1.48 : 1.64	1.00 : 1.00 : 1.28
9×9	162	1.00 : 1.58 : 1.57	1.08 : 1.00 : 1.29

Algorithm 3 RCA Optimised Independent Set CA

Input: $G = (V, E)$, $G_c = (V_c, E_c)$, $CS = \{1, 2, \dots, M\}$
Output: RCA OIS Channel Assignment For G

```

1:  $IS \leftarrow FindIndependentSets(G_c)$ .  $\{IS : \text{Set of mutually exclusive Independent Sets of vertices of } G_c.\}$ 
2:  $Channel \in CS$ ,  $Channel \leftarrow 1$ .
3: for  $IndSet \in IS$  do
4:   for  $Node \in IndSet$  do
5:      $Node \leftarrow Channel$ 
6:   end for
7:    $Channel \leftarrow Channel \% M + 1$ 
8: end for
   { Let  $V_r$  be the subset of all vertices in  $V_c$  which denote a link emanating from a particular radio  $r$  in  $G$ . Let  $C_{last}$  be the  $Channel$  assigned to the last element processed in  $V_r$ }
9:  $r \leftarrow C_{last}$  {Facilitates improvised vertex coloring}
10: for  $i \in V$  do
11:    $Num_i \leftarrow i$  {Number the nodes from  $(1, \dots, N)$ }
12:   Determine  $Ch_i$  and  $Adj_i$ 
13: end for
   {Ensure Topology Preservation in  $G$ }
14: for  $i \in V$  do
15:   for  $j \in Adj_i$  do
16:     if  $((Num_i < Num_j) \ \&\& \ (|Ch_i \cap Ch_j| == 0))$  then
17:        $Ch_j \leftarrow Ch_j + \{c_{com}\} - \{c_{dif}\} \mid \{(c_{com} \in Ch_i) \ \&\& \ (c_{dif} \in Ch_j) \ \&\& \ (TID(G) \text{ is minimum})\}$ 
18:     end if
19:   end for
20: end for
21: Perform Radio Co-location Optimization in  $G$  {Steps described in Algo 4}

```

6.3.1 RCA OIS-CA Algorithm

I now present RCA *Optimized Independent Set* or OIS, CA algorithm in Algo 3. Here, we approach the CA problem as an improvised vertex-coloring problem ensuring that no radio on any node in the original WMN graph G is assigned multiple channels. For a smooth discourse, let us consider an arbitrary radio r in the WMN. All the wireless links emanating from this radio will be represented in the E-MMCG G_c by a subset of vertices V_r , that will form a *clique* as every vertex element in V_r will be connected to every other vertex in the subset. The initial step is to partition the vertex set of the E-MMCG into ISs. This is done by traversing each node exactly once, and allotting it an IS. If a node can not be assigned to any of the existing ISs, a new IS is created of which it becomes the first node. If a node can be assigned to more than one ISs, an IS is chosen at random. Next, all nodes of an IS are assigned the same channel, and the channel to be assigned to the next IS is selected in

a cyclic fashion. But, any two vertices in the clique V_r will never be a part of the same IS as they are pair-wise adjacent to each other in the E-MMCG, and this very fact forbids translating the CA problem into a corresponding simple vertex coloring problem. To overcome this handicap, we adopt a *selective* vertex coloring approach. As all the vertices in V_r will lie in different ISs, depending upon the number of available channels and the cyclic channel assignment, they may or may not have been assigned different channels. Thus, after generating all the ISs we identify the color (channel) that has been assigned to the elements of V_r the maximum number of times, and assign the radio r in G that particular channel. If all colors (channels) have been assigned an equal number of times or all elements in V_r have been assigned different colors, we pick a color (channel) randomly and assign it to r . The insight behind this improvisation is that a vertex in E-MMCG represents a link between two radios, and allocating radio r a channel that has been assigned to maximum number of vertices in V_r will ensure increased connectivity in the WMN graph after CA exercise. From a computational perspective, the cyclic manner of assigning channels to ISs facilitates an $O(1)$ time implementation of the selective vertex coloring approach by leveraging the idea that the color (channel) assigned to the last element in V_r denoted by C_{last} , will always be one of the maximally assigned channels among the vertices of V_r .

Despite being designed to achieve improved connectivity in the WMN, the initial OIS-CA may disrupt the original WMN topology, and may even lead to a disconnected graph G . It is thus of great importance to preserve the original WMN topology which reflects the intended physical span of the wireless network. Designing a generic topology preserving optimal CA algorithm is an established NP-hard problem [37]. Hence, the algorithm described in steps 10 – 20 of Algo 3 is a smart heuristic approach specifically tailored to ensure topology preservation after the initial channel assignment. The algorithm first sequentially orders the nodes of the WMN graph G , and assigns every node i a number Num_i . It then determines for each node i in G , the sets (Ch_i) and (Adj_i) . Further, for every i in G , every neighboring node j in Adj_i such that $Num_i < Num_j$, is scanned to determine if i & j share a common channel to communicate. If not, then the WMN topology is violated, and a *forward correction* technique is adopted to establish a connection between the two nodes and restore the topology. The constraint $Num_i < Num_j$ ensures that in every topology preserving channel re-assignment, a channel from node i is picked and assigned to node j *i.e.*, a correction in the forward direction, thereby forbidding the possibility of a backward link disruption on a node while attempting to re-establish its connection on another link. Further, the choice of the (c_{com}, c_{dif}) pair, from Ch_i and Ch_j respectively, is predicated on a minimum TID value or a maximum decrease in the estimate of the prevalent interference.

The final and the most crucial step involves radio co-location interference mitigation, a performance enhancement feature which is the combined outcome of the use of E-MMCG model for initial channel assignment, and the post channel allocation radio co-location optimization function. Thus, the twin methods of restraining RCI have been employed in conjugation.

6.3.2 Radio Co-location Optimization

Radio co-location optimization functionality presented in Algo 4 commences by ascertaining Ch_i and Adj_i for each node i of G . It explores Ch_i of each node to determine if two or more spatially co-located radios (*SCRs*) have been assigned an identical channel to operate on. If so, it attempts to alleviate the RCI by re-assigning all such *SCRs* barring one, distinct channels from the set of

Algorithm 4 Radio Co-location Optimization

Input: $G = (V, E)$, $CS = \{1, 2, \dots, M\}$ **Output:** Mitigate RCI in G & minimize $TID(G)$

```
1: for  $i \in V$  do
2:   Determine  $Ch_i$  and  $Adj_i$ 
3: end for
4: for  $i \in V$  do
5:   if  $((j_1, j_2, \dots, j_k, Channel) \in Ch_i) \ \&\& \ (j_1 = j_2 = \dots = j_k = Channel)$  then
6:      $j_1 \leftarrow Channel, j_2 \leftarrow c_2, \dots, j_k \leftarrow c_k | \{((c_2, \dots, c_k) \in CS \text{ are distinct if possible}) \ \&\& \ (TID(G) \text{ is minimum})\}$ 
7:   end if
8: end for
9: for  $i \in V$  do
10:  for  $j \in Adj_i$  do
11:    Get  $c_{ij}$  {Current channel of wireless link  $(i, j)$ }
12:    for  $c_{dif} \in CS$  do
13:      if  $((c_{ij} \leftarrow c_{dif}) \ \&\& \ (NetTopoPreserved())) \ \&\& \ (TID(G) \text{ decreases})$  then
14:         $Ch_i \leftarrow Ch_i + \{c_{dif}\} - \{c_{ij}\}$ 
15:         $Ch_j \leftarrow Ch_j + \{c_{dif}\} - \{c_{ij}\}$ 
16:      end if
17:    end for
18:  end for
19: end for
```

all available channels (CS) ensuring that the final configuration results in a minimum TID value. One of the SCRs continues to operate on the channel it was originally assigned so as not to disrupt an existing wireless link of the node in context. After performing RCI mitigation, the function analyzes each wireless link of the WMN exactly once, to check if the current channel of the link can be replaced with an alternate channel (c_{dif}) from CS so that the overall TID estimate decreases and with an important caveat that the underlying WMN topology is preserved denoted by function ($NetTopoPreserved()$). If a desirable channel replacement for a link is found, the current channel (c_{ij}) connecting the nodes i & j is removed from both Ch_i & Ch_j , and the preferred channel (c_{dif}) is added to both.

The features described above, coupled with the characteristic that the ISs are generated concurrently in OIS-CA result in ISs of comparable cardinalities. In sharp contrast cardinalities of MISs generated consecutively, as in MaIS-CA, fail to provide for a balanced distribution of channels among radios. Table 9.1 illustrates the performance of RCA OIS CAs in terms of statistical evenness. OIS outperforms MaIS, and the following two aspects elicit this observation. Firstly, in OIS the difference between the cardinalities of any two sets of radios among R_{C1} , R_{C2} & R_{C3} , never exceeds 35% and the difference between at least a pair of mentioned sets is always under 10%. This ensures a balanced channel assignment. Secondly, the default channel C_1 is not under utilized and is assigned to almost as many radios as channel C_2 , occasioning and guaranteeing fairness in spectrum utilization. The relevance of an even statistical distribution, and fairness in channel utilization demonstrated by RCA OIS-CA is vindicated by the TID estimates depicted in Figure 6.1. The grid WMNs are of size $(N \times N)$, where $N \in \{3, \dots, 10\}$, each node is equipped with 2 radios and 3 orthogonal channels are available. It can be inferred from the consistently lower TID estimates exhibited by RCA OIS-CA, as compared to MaIS-CA, that it is the more efficient CA scheme owing to its intelligent algorithm

design. This theoretical conclusion will be substantiated by the experimental results presented in later sections.

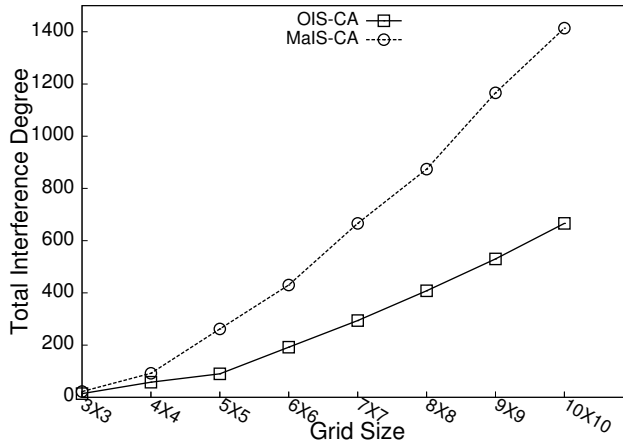


Figure 6.1: TID values of RCA OIS-CA vs MaIS-CA

6.4 Elevated Interference Zone Mitigation (EIZM) CA

I now propose the RCA *EIZM* algorithm pivoted primarily on the spatial characteristics of the endemic radio interference, but which factors in the statistical dimension as well. The motivating principle catalyzing the algorithm design is that the intensity of prevalent interference fluctuates within a wireless network, causing localized pockets of unusually high interference levels. We call the wireless links in the WMN which form the epicenter of such severe *performance bottlenecks* as the *Elevated Interference Zones* or EIZs. Taking a cue from the study on the impact of interference on a WMN in [38], we offer the argument that the EIZs impede the network performance drastically as they substantially degrade the *signal to noise plus interference ratio* (SINR) on neighboring links in the network. A WMN having a large number of links on which a data transmission experiences strong levels of interference, even though the communication over the remaining links exhibits a high SINR, will lead to a dismal aggregate network capacity owing to the inherent multi-hop nature of packet exchange among nodes. In contrast, a WMN in which all radio links experience a lower SINR will perform better than the former. Thus an EIZ is a particular wireless link in the WMN that may cause severe degradation of the network capacity. The question now remains as to how do we precisely characterize an EIZ for an accurate physical modeling? We contend that a wireless link with a high number of adjacent links is a potential EIZ, the extent of whose severity is predicated upon the channels allocated to it, and its neighboring links. The intuitive notion for such consideration is that the channel assignment on an EIZ tends to have an enormous impact on the network performance due to a high number of potential conflict links. A favorable channel assigned to an EIZ may significantly improve the overall network capacity while an ill-chosen channel may exacerbate the effects of interference manifold. We adopt a view that eroding the detrimental impact of interference on an EIZ will occasion a ripple effect that will certainly reduce the adverse effects of interference on its adjacent links.

I now translate the theoretical proposition into a feasible practical implementation *i.e.*, correlate

the concept of an EIZ in a WMN with its representation in the E-MMCG. An EIZ in the WMN is identified by its corresponding node in the E-MMCG, and by labeling E-MMCG nodes as EIZs, the algorithm pinpoints the respective performance bottleneck links in the WMN. The RCA EIZM-CA algorithm accepts the E-MMCG of a WMN as input, and considers EIZs to be the nodes with the *maximal degree* and nodes which share the *maximal number of neighbors* with an existing EIZ. The maximal degree node signifies a link with the maximum link-adjacency in a WMN and an obvious reference EIZ node to begin with. The subsequently chosen EIZ nodes are those which share the most number of mutual neighbors with the existing EIZ node. The process of EIZ selection should ideally be based on the SINR values of nodes. However, SINR values are a temporal or dynamic link quality parameter and can be ascertained only during active data transmissions. Thus, the improvised EIZ selection approach considers the theoretical TID estimates as an approximate measure of the impact of interference instead of the dynamic SINR values, and nodes with high TIDs are the first candidates to be labeled EIZs. Further, the scheme intelligently assigns channels to the EIZ nodes so that the detrimental impact of interference on the WMN, represented by the TID estimate, reduces. This is a spatial algorithm design strategy wherein the intense EIZs *i.e.*, the maximal degree nodes in E-MMCG are efficiently assigned channels first. Thereafter the nodes which share the maximal number of mutual neighbors with them are visited and so forth, triggering an *outward ripple* of interference mitigation.

6.4.1 RCA EIZM-CA Algorithm

EIZM approach elucidated in Algo 5, employs a Breadth First Traversal (BFT) starting from a reference node, which could be a node representing a link to the Gateway or a specifically chosen node. We consider a maximal degree node $v_{maximal}$, which is unarguably an EIZ, to be the reference. A *Level Structure* (LS) is generated, which is a partition of the vertex set V_c into subsets of vertexes that lie in the same level of the BFT *i.e.*, vertices which are situated the same number of hop-counts away from $v_{maximal}$ are placed in the same level. We term these subsets of the LS as *level-sets*. Next, to fashion a fair spectrum utilization, each level-set is assigned a channel chosen from CS in a cyclic manner. This step caters to the statistical aspects of interference alleviation, by attempting to maintain an equitable distribution of channels across radios in the WMN. In addition, vertices of level-sets which differ by a single level are assigned non-overlapping channels, thereby substantially reducing link conflicts. The next step entails processing each level-set, and assigning channels to the nodes within a level-set, iteratively. The EIZs are identified in each level-set. When a level-set is being processed for the first time, the maximal-degree node in the level-set determined by the function *MaximalDegNode*, serves as the initial EIZ node. In subsequent iterations the function *MaximalMutualNeighbor* chooses the node which boasts of the highest number of mutual neighbors with the previous EIZ node to be the current EIZ node. If there is more than one node to pick from, the node with the highest degree among them is selected as the next EIZ. Thereafter, the EIZ node is re-assigned a channel from CS which results in a minimum TID value. This step may or may not alter the initial assignment, depending upon the TID estimate. Upon final assignment, the EIZ node is removed from the level-set and aids in identifying the next EIZ node. After the initial channel allocation the algorithm ensures topology preservation through the steps described earlier in OIS-CA implementation. The last and the most important step is the RCI optimization proposed in Algo 4, which has also already been elaborated upon.

Algorithm 5 RCA Elevated Interference Zone Mitigation CA

Input: $G = (V, E)$, $G_c = (V_c, E_c)$, $CS = \{1, 2, \dots, M\}$ **Output:** RCA EIZM Channel Assignment For G

```
1: Let  $v_{maximal} \leftarrow maximalDegNode(V_c)$ 
2:  $LS \leftarrow LevelStructure(v_{maximal}, G_c)$  { $LS$  : Set of level-sets generated by Breadth First Traversal
   of vertices of  $G_c$ }
3:  $Channel \in CS$ ,  $Channel \leftarrow 1$ 
4: for  $LevSet \in LS$  do
5:   for  $Node \in LevSet$  do
6:      $Node \leftarrow Channel$ 
7:   end for
8:    $Channel \leftarrow Channel \% M + 1$ 
9: end for
10: for  $LevSet \in LS$  do
11:    $PrevNode_{EIZ} \leftarrow 0$ 
12:   for  $Node \in LevSet$  do
13:     if ( $PrevNode_{EIZ} \leftarrow 0$ ) then
14:       Let  $Node_{EIZ} \leftarrow maximalDegNode(LevSet)$  {Maximal degree node in the Level Set is the
         initial EIZ node}
15:     else
16:       Let  $Node_{EIZ} \leftarrow$ 
          $MaximalMutualNeighbor(LevSet, PrevNode_{EIZ})$ 
17:     end if
18:      $Node_{EIZ} \leftarrow Channel$ , such that  $TID(G)$  is minimum
19:      $PrevNode_{EIZ} \leftarrow Node_{EIZ}$ 
20:      $LevSet \leftarrow LevSet - \{Node_{EIZ}\}$ 
21:   end for
22: end for
23: Ensure Topology Preservation in  $G$  {Perform steps 10 to 20 described in Algo 3}
24: Perform Radio Co-location Optimization in  $G$  {Steps described in Algo 4}
```

The illustrations presented in Figure 6.2 provide an insight into the functioning of the EIZM algorithm. Figure 6.2 (a) is an E-MMCG representation of a sample WMN in which the reference node signifies a corresponding link to the Gateway in G , and is denoted by GW . Based on the proposed characteristics of an EIZ, the primary potential EIZ candidates are nodes B and D , and upto a lesser extent, nodes C and F . This inference is substantiated by the sequence of EIZ node identification carried out by EIZM scheme, depicted in Figure 6.2 (b). The number in the subscript of the node label is the sequence number of the order in which EIZ node were identified. The algorithm considers GW as the reference and performs a BFT, yielding B, D, C, A as the elements of the 1st level-set *i.e.*, the set of nodes one hop away from GW . Nodes of the 1st level-set are linked to GW through dotted lines in Figure 6.2 (b). As expected, node B is the 1st EIZ, followed by C , D and A . The 2nd level-set which comprises of all the remaining nodes, produces the sequence F, G, E, H and I of consecutive EIZ nodes. It may be argued that A was chosen as an EIZ before F , despite the latter exhibiting stronger EIZ characteristics. The underlying reason is that node A is one hop away from GW , an element of the 1st level-set, and thus processed before C which lies in the 2nd level-set. This however, is not an anomaly but a consequence of a conscious design choice to divide the E-MMCG nodes into level-sets. This technique serves the twin objectives of a fair distribution of channels among radios, and because of the channel initialization of each level-set in a cyclic manner, it ensures minimal conflict between nodes of consecutive level-sets, diminishing

impact of interference. Hence, the EIZM algorithm maintains a fine balance between the spatial and statistical aspects of interference mitigation, and benefits by doing so.

The BFT approach is quite often used in CA schemes. For example in the BFS-CA algorithm suggested in [20], a BFT is performed on the multi-radio conflict graph or MCG of the WMN, starting from a Gateway node. The nodes are accessed in the increasing order of hop-count from the Gateway, and assigned channels. However, BFS-CA and other BFT based algorithms, do not take into account the existence of high interference zones, and hence do not prioritize their channel assignment based on the EIZ concept. Secondly, although BFS-CA processes nodes on the basis of hop-counts, it does not initialize nodes situated one hop-count away from each other with different channels. Thus, it fails to facilitate a balanced and fair channel distribution. Finally, like all other CA schemes, BFS-CA too fails to acknowledge RCI and take measures to alleviate it. Experimental results will demonstrate that EIZM scheme, designed in conformity with the proposed concepts, registers a network capacity which is even more than 2.5 times that of BFS-CA for a few test scenarios.

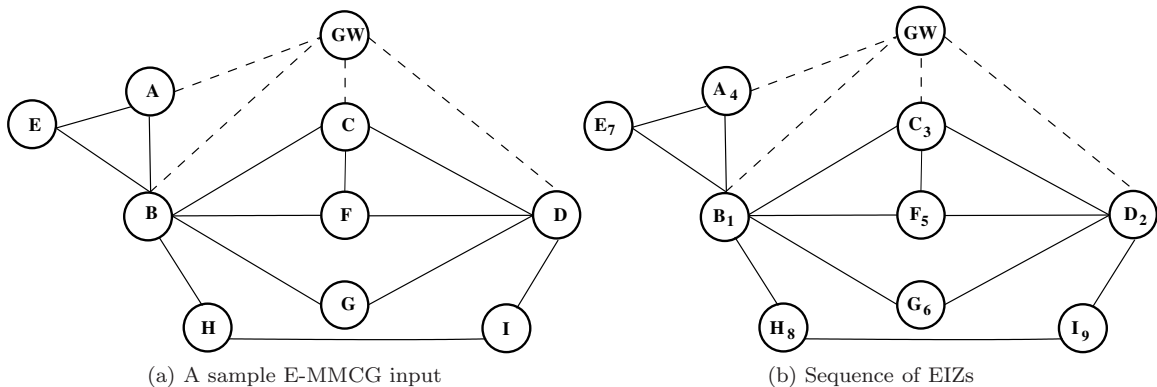


Figure 6.2: EIZ selection in *EIZM-CA*

6.5 Time Complexities Of Proposed Algorithms

For a given a WMN graph G of n nodes and its E-MMCG G_c of m nodes, we suggest the computational costs of the proposed RCA CA schemes. Since both OIS-CA and EIZM-CA accept the E-MMCG G_c as input, their time complexities are a function of m . In OIS-CA, generating the ISs takes $O(m^2)$ time, as does the BFT in EIZM-CA. In contrast, the topology preservation technique operates on WMN graph G as input. It first numbers the nodes in G and then for each node, traverses its adjacent nodes. Thus it has a worst-case cost of $O(n^2)$. Similarly, it can be derived that radio co-location optimization function has $O(n^2)$ complexity as well. However, due to high number of conflict links in a MRMC WMN, the number of nodes in the E-MMCG are much greater than those in the original WMN *i.e.*, $m \gg n$. Thus, it is reasonable to conclude that the overall time complexity of both the RCA CA algorithms is $O(m^2)$.

Chapter 7

Performance Evaluation of Radio Co-location Aware Channel Assignments

It is imperative that we prove the relevance of the proposed RCA CA schemes and validate the arguments their design is predicated on, through extensive experimental results. The objectives are two-fold.

- **Demonstrate the significance of Radio Co-location Optimization** : We highlight that RCI optimization functionality does substantially enhance a CA's performance, consolidating the primary premise this study is based on. This is accomplished by comparing the instance of the proposed CA schemes that is non-RCA *i.e.*, the CA generated before radio co-location optimization step, with the corresponding final RCA CA. The RCA CAs are denoted by *OIS-CA* & *EIZM-CA* while their non-RCA counterparts are represented by *OIS-N-CA* & *EIZM-N-CA* in the result illustrations.
- **Compare performance of RCA CAs with conventional CAs** : We present experimental evidence to corroborate that RCA CAs significantly outperform the conventional CAs that do not ensure RCI alleviation and lack a spatio-statistical design. We employ MaIS-CA [31] and BFS-CA [20], as the reference CAs against which we compare OIS-CA and EIZM-CA, respectively. The reference CAs are carefully chosen to demonstrate that despite a likeness in the underlying approach of the CA pairs OIS-CA & MaIS-CA, and EIZM-CA & BFS-CA, elaborated upon earlier, the RCA algorithms fare remarkably better.

7.1 Simulation Setup

We perform exhaustive simulations in ns-3 [15] to gauge the performance of CAs deployed on the following two WMN topologies.

- 5×5 grid WMN depicted in Figure 7.1.
- A random WMN of 50 nodes spread across an area of $1500m \times 1500m$.

7.1.1 Simulation Parameters

The choice of a grid WMN is motivated by the fact that they fare better than random layouts in terms of coverage area and mesh network capacity [39], resulting in an ideal topology for CA performance

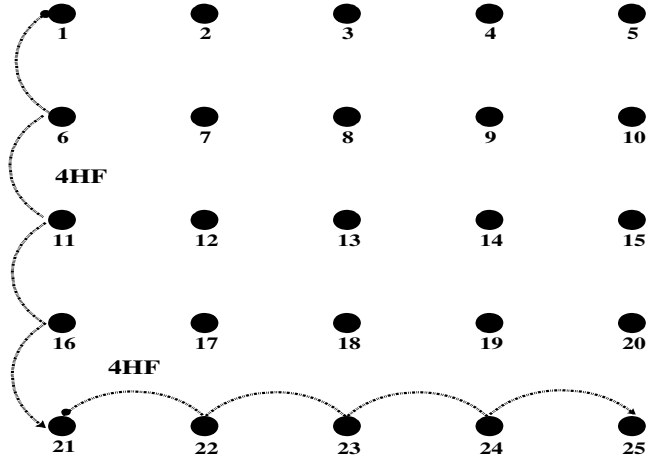


Figure 7.1: A 5×5 grid

evaluation. The simulated environment of a large WMN comprising of 50 randomly placed nodes is also a relevant layout, as it resembles a real-world WMN deployment which is less likely to conform to a grid pattern. The large number of nodes spread over a wide area facilitates long distance data transmissions requiring multiple-hops between nodes placed on the fringes of the network, a scenario vital for estimating the efficiency of a CA in performing such transmissions. For ease of reference, grid WMN and random WMN are abbreviated as *GWMN* and *RWMN*, respectively. The simulation parameters are presented in Table 7.1. Each multi-hop traffic flow transmits a datafile from the source to the destination. For the grid WMN, we equip each node with 2 radios and CA schemes have 3 orthogonal channels at their disposal. Given the enormity and complexity of the random WMN we scale up the technical specifications. Thus each node has 3 radios, and each radio can be allotted one of 4 orthogonal channels. We carry out two set of simulations employing TCP and UDP as the underlying transport layer protocols. We leverage the inbuilt ns-3 models of *BulkSendApplication* and *UdpClientServer* for TCP and UDP implementations, respectively. TCP simulations are aimed at estimating the *Aggregate Network Throughput*, which we henceforth simply refer to as the *Throughput*, for each scenario. UDP simulations are employed to determine the *packet loss ratio* (PLR) and the *mean delay* (MD) for a test-scenario.

7.1.2 Data Traffic Characteristics

Tailoring an ideal set of *data traffic characteristics* is a crucial step so as to aptly highlight the performance bottlenecks caused by the endemic interference and to explicitly demonstrate the mitigation of their adverse impact on the WMN performance by the deployed CA. Since, multi-hop data flows are an inherent feature of WMNs, we simulate a variety of test scenarios for both the WMN topologies which employ the following multi-hop flows.

Grid WMN

4-Hop Flows or 4HFs are established from the first node (source) to the last node (sink), of each row and each column of the grid. 8-Hop Flows or 8HFs are set up between the diagonal nodes of the grid.

Table 7.1: ns-3 Simulation Parameters

Parameter	Value
Radios/Node	GWMN: 2, RWMN: 3
Range Of Radios	250 mts
IEEE Protocol Standard	GWMN: 802.11g RWMN: 802.11n
Available Orthogonal Channels	GWMN: 3 (2.4 GHz) RWMN: 4 (5 GHz)
Transmitted File Size	GWMN: 10 MB RWMN: 1 MB
Maximum 802.11g/n Phy Datarate	54 Mbps
Maximum Segment Size (TCP)	1 KB
Packet Size (UDP)	GWMN: 1 KB RWMN: 512 Bytes
MAC Fragmentation Threshold	2200 Bytes
RTS/CTS	Enabled
Packet Interval (UDP)	50ms
Routing Protocol Used	OLSR
Loss Model	Range Propagation
Rate Control	Constant Rate

Random WMN

We create a plethora of multi-hop flows between nodes which are 3 to 10 hops away, ensuring that the paths of many of these flows intersect to occasion comprehensive interference test-scenarios.

7.1.3 Test Scenarios

Various combinations of the multi-hop flows described above are devised to generate test-scenarios, that reflect both, a *sectional* view and a *comprehensive* view, of the intensity, impact and alleviation of the prevalent interference. Test-cases for both the WMN layouts are listed below.

Grid WMN

1. $D2$: Both 8HDFs concurrently.
2. $H5$: All five 4HF's concurrently in the horizontal direction.
3. $V5$: All five 4HF's concurrently in the vertical direction.
4. H_4V_4 : Variety of eight concurrent flows, which include various combinations of 4HF's.
5. $H5V5$: Ten concurrent 4HF's *viz.* H5 & V5.
6. $H5V5D2$: Twelve concurrent flows. *viz.* D2, H5 & V5.

Test cases (a, b & c) offer a directional perspective of CA performance, while scenarios (c, d & e) form the exhaustive benchmarks on which the overall performance of CA can be assessed.

Random WMN

Given the random placement of nodes, the test-scenarios include a combination of concurrent multi-hop flows of varying hop counts. 4, 8, 12, 16 and 20 concurrent multi-hop flows were established, where the number of simultaneous data flows represents a test-case *viz.* TC_4 , TC_8 , TC_{12} , TC_{16} & TC_{20} . As the number of concurrent flows increases, the interference dynamics become more

complex. Thus test-cases TC12, TC16 and TC20 are ideal to gauge CA efficiency in terms of network performance metrics.

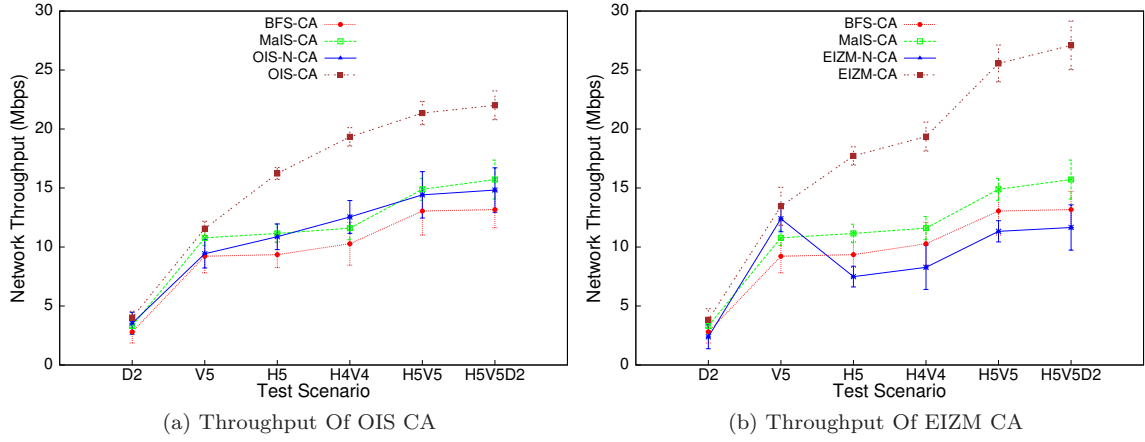


Figure 7.2: Aggregate GWMN Throughput

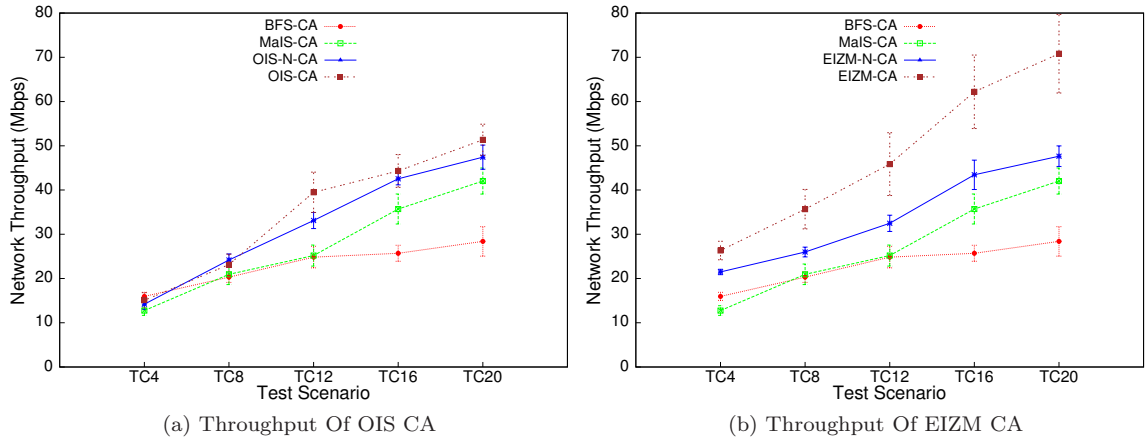


Figure 7.3: Aggregate RWMN Throughput

7.2 Results and Analysis

Rigorous simulations were run for the test-cases described above, and the observed values of performance metrics *viz.* Throughput (Mbps), PLR (% of packets lost) and MD (μ seconds) are now presented for a thorough analysis of the performance of the proposed RCA CAs.

7.2.1 Throughput

The throughput results for simulations run on GWMN and RWMN topologies are depicted in Figures 7.2 & 7.3. For statistical reliability *99% Confidence Interval* bars have been marked for the recorded Throughput value of each test-case. The first objective is met through a conspicuous inference from the listed plots, that the non-RCA version of the proposed CAs registers much lower

throughput than the RCA version, highlighting the efficacy of radio co-location optimization feature of the RCA CAs and consolidating the theoretical contention that RCI mitigation enhances the network capacity significantly. EIZM-CA registers a maximum capacity enhancement of 132% for scenario H5V5D2 in GWMN and about 48% for scenario TC20 in RWMN, over EIZM-N-CA. Improvements exhibited by OIS-CA over OIS-N-CA for identical scenarios are 48% and 8%, respectively. Let us now analyze the performance of the RCA CAs in comparison to the reference CAs. Its discernible that RCA CAs outperform both MaIS-CA and BFS-CA by a significant margin. This is evident from the substantial increase in Throughput in RCA CA deployments, displayed in Table 7.2.

Table 7.2: Enhancement in network capacity through RCA CAs

Comparing CAs	% increase in Throughput in TC			
	TC16	TC20	H5V5	H5V5D2
EIZM-CA vs BFS-CA	142	149	96	106
EIZM-CA vs MaIS-CA	74	68	72	72
OIS-CA vs BFS-CA	72	81	64	67
OIS-CA vs MaIS-CA	24	22	43	40

EIZM-CA turns out to be the better of the two high performance RCA CAs, however OIS-CA fares quite better than both BFS-CA and MaIS-CA as well. Another interesting observation is that the non-RCA CAs perform decidedly better than both of the reference schemes in the RWMN simulations, but not in the GWMN. Hence, no definitive conclusions can be made between non-RCA CAs and the the reference CAs, which highlights the importance of RCI alleviation in enhancing CA performance. Further, OIS-N-CA performs slightly better than OIS-CA in test-case TC8 in RWMN. However, this scenario projects a partial or sectional view of the RWMN and the upset in results does not amount to a reversal in the expected trend. This momentary aberration is remedied in the remaining test-cases, where OIS-CA continues to outperform OIS-N-CA. Another noteworthy point is the spatial impact of interference in GWMN where the scenarios H5 and V5 include an equal number of (five) concurrent 4HFs, along the rows and columns of the grid, respectively. Yet in Figure 7.2 (b) it can be observed that for EIZM-CA, scenario H5 records a higher throughput than V5 *i.e.*, lower impact of interference is experienced by transmissions along the rows, while for EIZM-N-CA the situation is reversed *i.e.*, transmissions along the columns register higher throughput.

7.2.2 Packet Loss Ratio

PLR performance metric observations are in absolute conformity with the network capacity results. For the RWMN layout, we present PLR for all the test-cases, however for the GWMN topology, results of the three comprehensive test-cases *viz.*, H4V4, H5V5 and H5V5D2, are presented as the PLR in other scenarios was negligible. In Figures 7.4 and 7.5, it can be noticed that both the RCA CAs experience the minimum packet loss. Similar to the result trends in throughput, RCA versions of CA show higher resilience to interference induced packet loss, leveraging the benefits of RCI mitigation functionality. Thus, PLR estimates also highlight the enhancement in performance of deployed RCA CAS owing to their twin capabilities of RCI alleviation and spatio-statistical design. For a quantitative analysis, the % reduction in PLR effected by RCA CAs in comparison to the

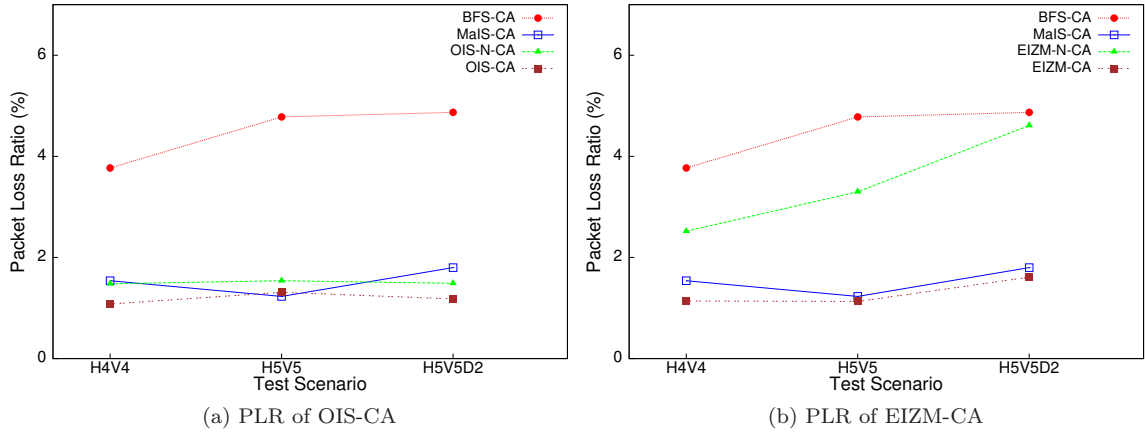


Figure 7.4: PLR of RCA CAs in GWMN

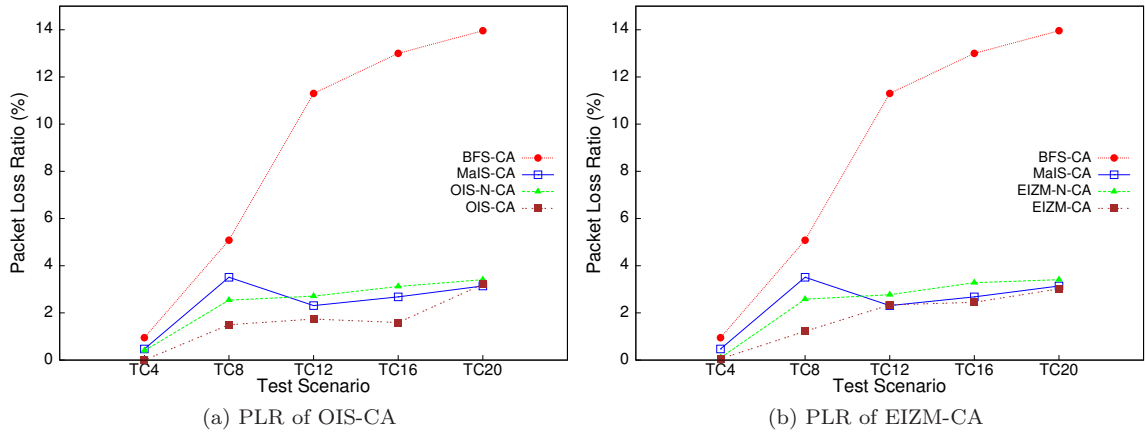


Figure 7.5: PLR of RCA CAs in RWMN

reference CA approaches is elicited in Table 7.3. There are three minor upsets in the observed

Table 7.3: Reduction in PLR through RCA CAs

Comparing CAs	% decrease in PLR in TC			
	TC16	TC20	H5V5	H5V5D2
EIZM-CA vs BFS-CA	81	78	76	67
EIZM-CA vs MaIS-CA	9	4	8	11
OIS-CA vs BFS-CA	88	77	73	76
OIS-CA vs MaIS-CA	41	-2	-6.5	34

trends, two between OIS-CA and MaIS-CA, where the latter performs marginally better in test cases TC20 and H5V5. But these slight reversals are mere exceptions in the observed pattern, and do little to discredit the improvement exhibited by RCA CAs. Further, between the two RCA CAs, EIZM-CA proves to be the better scheme in terms of packets lost during transmission.

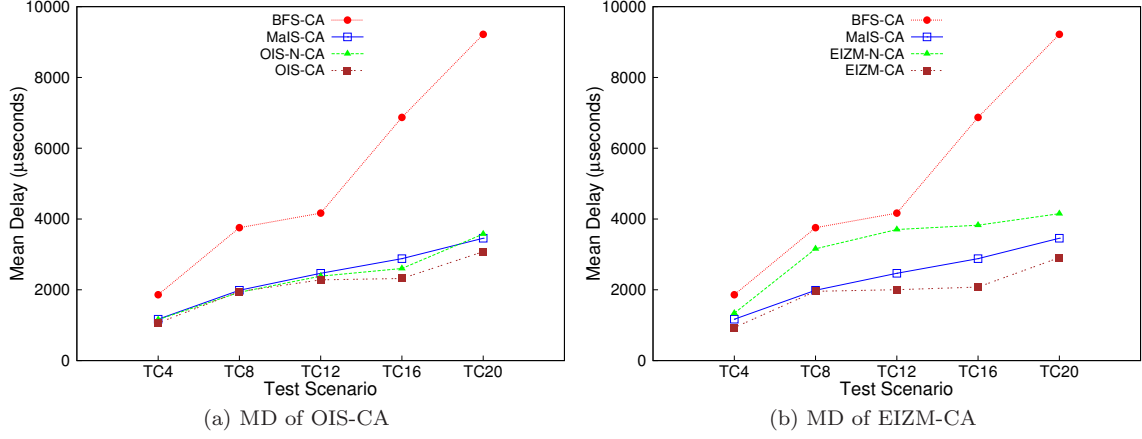


Figure 7.6: MD of RCA CAs in RWMN

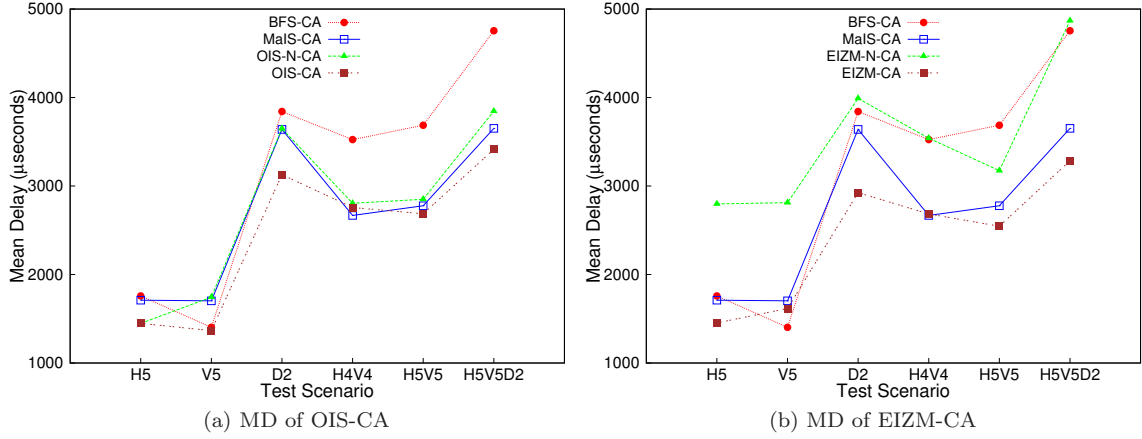


Figure 7.7: MD of RCA CAs in GWMN

Table 7.4: Reduction in MD through RCA CAs

Comparing CAs	% decrease in MD in TC			
	TC16	TC20	H5V5	H5V5D2
EIZM-CA vs BFS-CA	70	68	31	31
EIZM-CA vs MaIS-CA	28	16	8	10
OIS-CA vs BFS-CA	66	67	27	28
OIS-CA vs MaIS-CA	19	11	3	6

7.2.3 Mean Delay

Multi-hop flows are an inherent characteristic of the WMNs, hence it is of great relevance to observe the ease with which, for a CA implementation, data is transmitted across distant nodes in the WMN that are numerous hop-counts apart, especially under high network traffic loads. The recorded MD values are illustrated in Figures 7.7 and 7.6, for simulations run on GWMN and RWMN topologies, respectively. The delay characteristics of all the CAs are similar to those observed in PLR results. RCA CAs reduce the MD time considerably, especially in comparison to BFS-CA where the % reduction in delay times for scenario TC20 is 67% and 68% for OIS-CA and EIZM-CA, respectively.

This observation follows from the notion that a low PLR generally leads to a small packet delays. There are no noticeable reversals and RCA CAs consistently perform better than the reference CAs. Further, between the two RCA CAs, none has a distinct edge over the other. While OIS-CA exhibits small delay times for some test- cases, EIZM-CA registers a greater reduction in MD for others.

7.3 Summary

Having thoroughly deliberated over the performance of RCA CAs, we now make some sound logical conclusions. First, RCI prevalent in a WMN has a significant adverse impact on the network capacity, and its mitigation leads to enhanced Throughput and reduced PLR in a wireless network. Thus RCI mitigation ought to be a primary consideration in a CA scheme. Second, a prudent CA design that is tuned to the spatio-statistical aspects of interference alleviation will be more effective in restraining the detrimental effects of interference. Further, a CA scheme which caters to both spatial and statistical dimensions, such as EIZM-CA, stands to fare quite better than one which considers only one of the aspects in its design, such as OIS-CA. On the subject of the performance of the proposed RCA CAs, it can be unarguably concluded that they are significantly better than the reference CA schemes in terms of Throughput, PLR and MD. They are high-performance CAs which enhance network capacity tremendously, are resilient to packet loss, and reduce data propagation delays. Considering the average, EIZM-CA outperforms OIS-CA in terms of network capacity, by 45% and 11% in RWMN and GWMN layouts, respectively. The two RCA CAs are at par with respect to packet mean delay and PLR. The better performance of OIS-CA in GWMN can be attributed to the structured layout of a grid which facilitates a proportional distribution of channels across radios, unlike RWMN which is a large network of randomly placed nodes. EIZM-CA registers high performance in both WMN topologies, regardless of the layout. Clearly, EIZM-CA is the more efficient and better performing CA algorithm of the two, which it owes to its spatio-statistical design coupled with the feature of RCI mitigation. These findings provide an experimental validation to the emphasis we have laid on the spatio-statistical design of CA algorithms which is further improved through RCI alleviation measures.

Chapter 8

Total Interference Degree : A Reliable Metric ?

The theoretical measure of *Interference Degree* can be both *local i.e.*, of an individual node, and *total i.e.*, of a CA scheme in entirety [40]. This concept has been generously used in the WMN research literature to efficiently solve research problems such as the CA problem, the routing and scheduling problems etc [41]. With respect to the CA problem, the guiding idea is that a CA with lesser TID, will be more efficient and register better performance as compared to a CA with a higher TID [34]. However, we have observed that this theoretical idea does not always hold true when compared to the actual experimental data. In any domain relying primarily on experimentation and actual deployments, the proposed theories are seldom accurate or precise. Thus there is an acceptable threshold of deviation of real-time performance from the theoretical predictions. But in the case of TID of CAs, we contend that the reasonable threshold of acceptance is breached. In this chapter, we elaborate upon this problem.

8.1 Inadequacy of TID Estimates : An Example

On the basis of recorded network metrics, we now arrange the four CAs in the following sequence of decreasing performance : MaIS-CA₂ > MaIS-CA₁ > BFS-CA₂ > BFS-CA₁. Further, let us observe Table 5.1 again, and consider the TID values of CAs for the 5 × 5 WMN grid. Earlier we had compared the TIDs of two CAs belonging to the same MMCG model and made theoretical inferences. Instead of that, now if we consider the TID values of all four CAs irrespective of the MMCG model, the theoretical order of expected performance based on the TID values would be : MaIS-CA₁ > BFS-CA₁ > MaIS-CA₂ > BFS-CA₂. It is clear that this theoretical sequence is not in conformity with the established experimental sequence. A counter-argument may be presented that since a particular MMCG model was employed to compute the TIDs only for the CAs of the same model, a comparison of cross-model TID values is not logical. Hence, for a consistency in the approach taken to generate TID values, we employ the following two alternative methods to generate the TID values for all four CAs, regardless of the MMCG model they belong to.

1. Compute TIDs using the C-MMCG algorithm.
2. Compute TIDs using the E-MMCG algorithm.

I plot the computed TID values against the Throughput_{Net} values recorded in test-case FT-5 of *Test Case Class 2*, in Figure 8.1. The plot-lines for titles *C-MMCG* and *E-MMCG* correspond to the TIDs generated using the C-MMCG and the E-MMCG algorithm, respectively. The (*TID*,

$Throughput_{Net}$) co-ordinates for the CA quartet MaIS-CA₁, MaIS-CA₂, BFS-CA₁, BFS-CA₂ are labeled as M_1 , M_2 , B_1 and B_2 , respectively. Further, the C-MMCG plot labels are prefixed by a 'c', and the E-MMCG plot labels are prefixed by an 'e'.

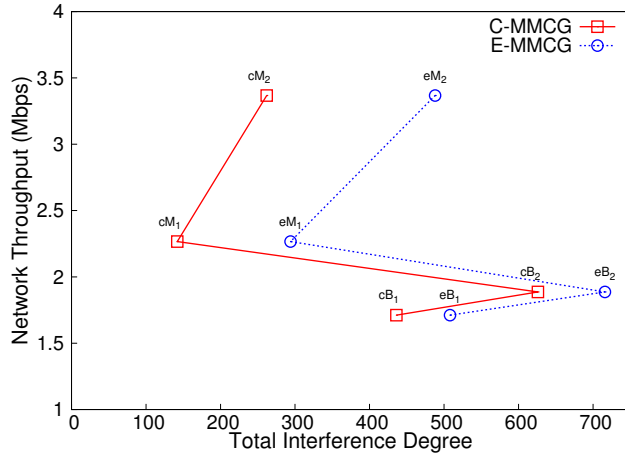


Figure 8.1: Correlation of TID with $Throughput_{Net}$ for FT-5

The plots for both the MMCG models are almost identical in shape and gradient, differing only in terms of the TID values. The E-MMCG CA versions register higher value of TIDs, which is expected as the model factors in the RCI scenarios too. Considering TID values to be the theoretical measure of expected performance, the sequence of CAs is the same for both methods : MaIS-CA₁ > MaIS-CA₂ > BFS-CA₁ > BFS-CA₂. Assuming that the TID estimates are a reliable measure of CA performance, the $Throughput_{Net}$ should decrease consistently with the rise in TID values, though not necessarily in a linear fashion. However, the two plots do not adhere to the expected pattern and exhibit a marked deviation which raises a valid concern about TID being a reliable theoretical metric to predict the performance of a CA.

8.2 Correlation Between TID and CA Performance

To validate this argument, we try to ascertain if there exists a strong correlation between the TID estimate of a CA and its performance in a given WMN.

8.2.1 Enlarged CA Sample Set

For a more comprehensive evaluation, we consider two more CA schemes in addition to BFS-CA and MaIS-CA. The first is a centralized heuristic scheme [30] which initially assigns a common channel to all nodes in the WMN. It then replaces the channels currently assigned to links so that the overall *interference number* of the network decreases *i.e.*, the TID of the WMN decreases. We denote it by *CEN-CA*. The second CA scheme is a maximal clique based approach [25], where the authors assign channels to radios in such a way that a *maximal clique* of the wireless links can be formed. Maximal clique creation would ensure that the number of non-conflicting links in a WMN is high. The CA scheme is represented as *CLQ-CA*. Further, we generate C-MMCG and E-MMCG variants for both CEN-CA and CLQ-CA, which are denoted in the naming convention being followed *i.e.*, CEN-CA₁ & CLQ-CA₁ are the C-MMCG CAs, while CEN-CA₂ & CLQ-CA₂ are their E-MMCG

counterparts. Thus, there are a total of 8 CA schemes and for each CA, we compute the TID and observe its performance in terms of Throughput_{Net} and PLR values.

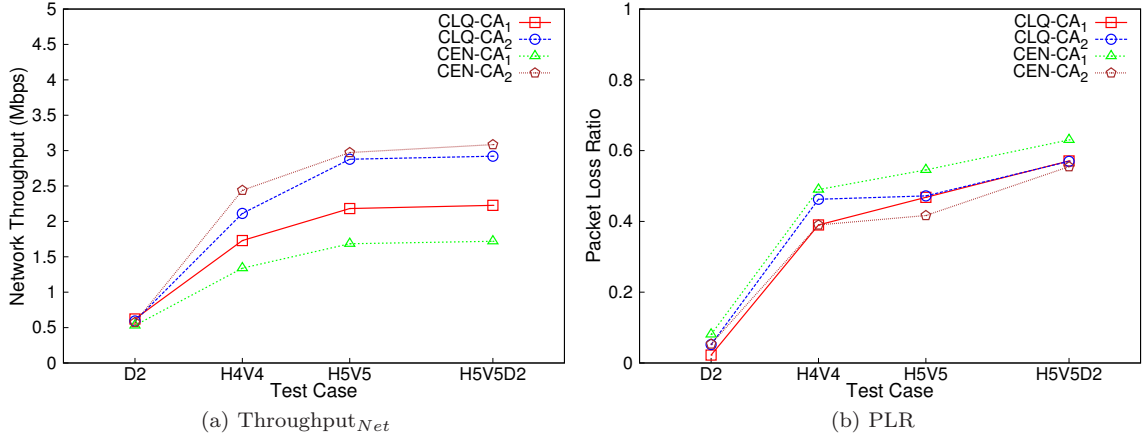


Figure 8.2: Performance of CEN-CA & CLQ-CA in Test Case Class 3

8.2.2 Performance of New CAs

I subject the CA set to the test-cases of Test Case Class 3, as these are the test scenarios of peak network traffic and thus ideal for assessing impact of interference on the recorded metrics. For each CA, we record the Throughput_{Net} and PLR values for the four test-cases *viz.*, D2, H4V4, H5V5 & H5V5D2. The results for BFS-CA and MaS-CA have already been presented in the previous section. We now present the Throughput_{Net} and PLR values registered for the new CAs in Figure 8.2 (a) and Figure 8.2 (b), respectively. Here too the E-MMCG CAs perform better than the corresponding C-MMCG CAs, both in terms of Throughput_{Net} and PLR. The only exception is CLQ-CA₂ registering a marginally higher PLR than CLQ-CA₁ in test-cases D2 and H4V4. Nevertheless, the four E-MMCG CAs perform decidedly better than their C-MMCG counterparts and these results further consolidate the efficacy of E-MMCG in restraining the RCI.

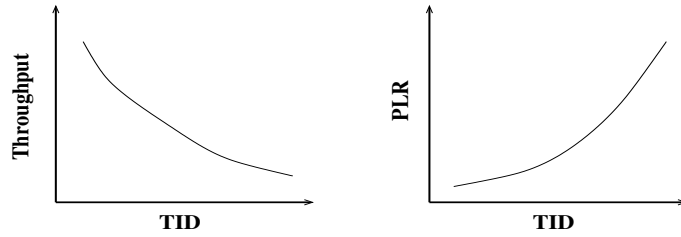


Figure 8.3: Expected correlation of TID with Throughput_{Net} and PLR

8.3 Comprehensive Evaluation of TID Prediction Accuracy

Next, we compute the average of the recorded Throughput_{Net} and PLR values of all the test-cases in Test Case Class 3, to determine the *Average (Avg) Throughput_{Net}* and *Average (Avg) PLR* for each CA. Average values of the two metrics reflect the overall performance of the CA in the grid

WMN topology, which can be compared with the TID value of the corresponding CA. The TID values are computed using the E-MMCG algorithm. The computed values of Avg Throughput_{Net} and Avg PLR are plotted against the TID values in Figures 8.4 (a) and 8.4 (b), respectively. The CA schemes are denoted as: BFS-CA₁ (BFS₁), BFS-CA₂ (BFS₂), MaIS-CA₁ (MIS₁), MaIS-CA₂ (MIS₂), CEN-CA₁ (CEN₁), CEN-CA₂ (CEN₂), CLQ-CA₁ (CLQ₁) and CLQ-CA₂ (CLQ₂). Higher

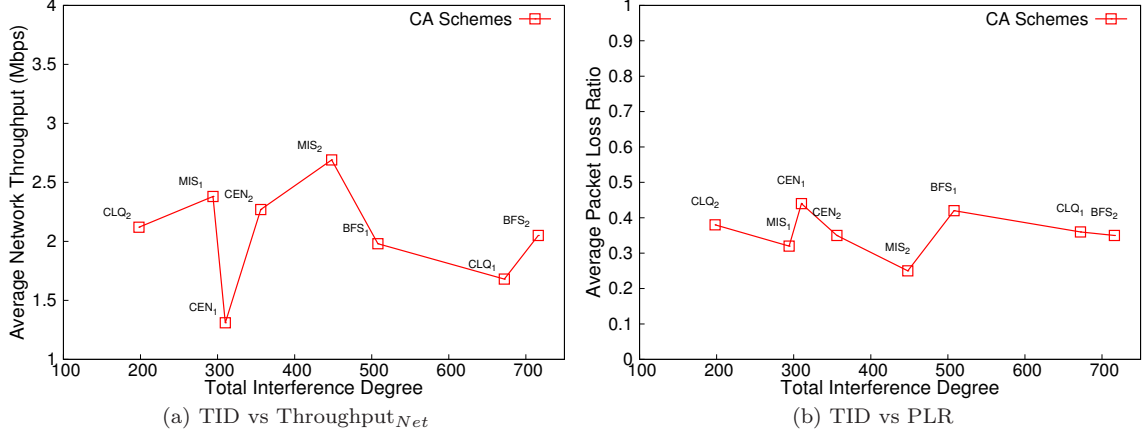


Figure 8.4: Correlation of TID with Network Performance Metrics

TID values suggest a greater adverse impact of interference. If we again assume TID estimates to be a reliable measure of CA performance, with increase in TID estimates the Avg Throughput_{Net} values must decrease while the Avg PLR values must rise. As depicted in Figure 8.3, the highest Avg Throughput_{Net} value should correspond to the CA with the lowest TID estimate and thereafter the plot should exhibit a negative gradient *i.e.*, a decrease in Avg Throughput_{Net} as the TID value increases. Likewise, the Avg PLR values should increase as the TID estimate increases *i.e.*, the plot should have a positive gradient. However, Figures 8.4 (a) & 8.4 (b) show marked deviations from the assumed trends. This is evident from the fact that CLQ-CA₂ has the lowest TID estimate among the 8 CAs while it ranks 4th in terms of Avg Throughput_{Net} and has the 3rd highest Avg PLR. In contrast, BFS-CA₂ has the highest TID value and yet offers a higher Avg Throughput_{Net} and lower Avg PLR than 3 other CAs. We now present the variation in CA sequences when arranged in the increasing order of expected performance on the basis of theoretical TID estimates, and the increasing order of actual performance on the basis of observed metrics. The CA sequences are elucidated below.

- **TID** : BFS-CA₂ < CLQ-CA₁ < BFS-CA₁ < MaIS-CA₂ < CEN-CA₂ < CEN-CA₁ < MaIS-CA₁ < CLQ-CA₂
- **Avg Throughput_{Net}** : CEN-CA₁ < CLQ-CA₁ < BFS-CA₁ < BFS-CA₂ < CLQ-CA₂ < CEN-CA₂ < MaIS-CA₁ < MaIS-CA₂
- **Avg PLR** : CEN-CA₁ < BFS-CA₁ < CLQ-CA₂ < CLQ-CA₁ < CEN-CA₂ < BFS-CA₂ < MaIS-CA₁ < MaIS-CA₂

It is clear that the CA performance sequence based on TID estimates is not in conformity with the CA performance sequences determined through experimental data. This finding will have profound

implications on the numerous CA approaches proposed in research literature which assume a direct correlation between TID estimate and CA performance. The underlying idea in most of these interference-aware CA approaches is to minimize the local interference degree at a node, or minimize the TID while assigning channels to WMN radios [34, 42].

8.4 Summary

There is no doubt that the theoretical concept of *Interference Degree* holds great relevance in estimating the intensity of prevalent interference at a node, or in an entire WMN. But extending this concept to compute *TID* for a particular CA in a WMN, and predicting the expected behavior or performance of the CA on the basis of its estimated TID value is not a practically accurate approach.

Chapter 9

Characterization and Estimation of Interference in Wireless Networks

9.1 Introduction and Related Research Work

The measure of the degradation of network performance by interference in a WMN deployment is intricately linked to the channel assignment (CA) scheme being employed. There is a multitude of CA schemes which can be implemented in any WMN deployment. However, selecting the most efficient and feasible CA from the enormous set of all CAs, for a given WMN of certain architecture and topology, is a tedious task. Further, there is an absence of CA performance prediction or estimation techniques in the research literature that could aid a network administrator in making this crucial choice. The conventional approach of estimating impact of interference in a WMN is to compute the total interference degree or *TID* [40][41], which equals half the sum of *interference degrees* of all the links in the graph representing a WMN. Here interference degree denotes the number of links that may potentially interfere or conflict with a given link. A TID estimate accounts for every potential conflict link in the WMN and is generated through its *conflict graph*. Thus, the TID estimate is an approximate measure of the endemic interference, and its magnitude is often assumed to be a reliable measure of the adverse impact of interference. For example, in interference-aware CA schemes, the guiding idea is to lower the TID to reduce the intensity of prevalent interference and make the CA more efficient [42]. However, in the previous chapter we have demonstrated that although TID does give a measure of the impact of interference, it is inconsistent and unreliable as a CA performance prediction, or interference estimation metric. Thus, we can not, with high confidence, compare two CAs or select the most efficient CA for a given WMN from a set of CA schemes by employing their TID estimates as the sole criterion for performance prediction.

Secondly, TID estimation is computationally expensive. Let $G = (V, E)$ represent an arbitrary MRMC WMN graph comprising of n nodes, where V is the set of nodes, E denotes the set of wireless links and each node is equipped with m radios. The complexity of determining the TID estimate is of the order $O(n^2m^3)$. This is because the adjacency relationships have to be established at the radio-to-radio granularity, for all nodes in V . Next, conflict links are determined for each radio-to-radio link in the WMN, leading to an algorithmic complexity of $O(n^2m^3)$.

In this chapter, we aim to remedy this problem by first proposing a fresh theoretical characterization of the interference prevalent in WMNs. We then suggest an intuitive statistical *interference estimation* or *CA performance prediction* technique, based on the proposed classification. Through

extensive simulations we demonstrate that the proposed metric is more reliable than the conventional TID metric. In addition, the proposed metric also consumes lesser computational resources.

9.2 A Fresh Characterization of Interference

The classification of interference in wireless networks is based on the *source* of the conflicting wireless transmissions on an identical channel. Thus, it is categorized into *internal*, *external* and *multi-path fading* [12]. However, this view is rather simplistic and fails to reflect the inherent *characteristics* which are intrinsic to all forms of interference affecting the wireless communication, regardless of their source or cause. We adopt a fresh approach to elicit these inherent characteristics of interference as they aid us in assessing and estimating its adverse impact on the network performance. We consider a single-gateway WMN model depicted in Figure 1.1, which comprises of mesh-routers (nodes) and mesh-clients. Multiple radios are available for inter mesh-router communication and we focus on the interference characterization of the mesh backbone. Next, to study these characteristics we consider a network scenario in which all nodes are active participants of multiple concurrent wireless transmissions. Each node functions as a source, or a destination, or an intermediate node relaying the data packets onto the next hop. As all nodes transmit in tandem, they trigger and intensify the intricate interference bottlenecks in a WMN, fashioning a prefect scenario in which interference can be considered to be a three dimensional entity, the dimensions being *temporal*, *spatial* and *statistical*. We now deliberate over this three dimensional model which constitutes the set of characteristics of the endemic interference.

1. **Temporal Characteristics** : These characteristics represent the *dynamism* in the interference scenarios. In a wireless network the transmissions are seldom synchronized, and on the contrary, are quite random. Thus, the interference complexities that are spawned in the network are a function of time and fundamentally temporal.
2. **Spatial Characteristics** : Link conflicts in a WMN are a result of two or more interfering links which are in close proximity. The links emanating from two radios transmitting on an identical channel would interfere *if and only if* they lie within each other's *interference range*. Consequently, this spatial interaction of wireless links is a fundamental feature of endemic interference.
3. **Statistical Characteristics** : The complexity of interference in a WMN is intricately linked to the assignment of available channels to the radios in the WMN. An even and judicious distribution of channels among radios will spawn fewer wireless conflicts as compared to a skewed distribution.

9.3 Interference Estimation & CA Performance Prediction

Interference estimation, alignment and cancellation are established NP-Hard problems [43]. A theoretical estimate of interference is only an approximate prediction of the WMN performance under a particular CA scheme. It helps to avoid the time and resource consuming task of ascertaining CA performance by implementing a CA in the WMN and carrying out real-time assessments. A TID estimate is the commonly used measure of the impact of endemic interference on WMN performance.

The TID metric only factors in the spatial aspects of interference by generating an estimate of the link conflicts, and does not take into account the other two dimensions. We employ the proposed characterization of interference to design an estimation algorithm which caters purely to a single dimension *i.e.*, the statistical aspects of interference, and offers a more reliable metric than TID.

9.3.1 A Statistical Interference Estimation Approach

We propose a scheme predicated on the notion of *statistical evenness* of channel allocation, which postulates that a proportionate distribution of the available channels among the radios will occasion an efficient CA. An even distribution of channels among radios in a WMN ensures fairness and boosts performance, as demonstrated in Chapter 7. We name it the *Channel Distribution Across Links* or *CDAL* algorithm. The name is indicative of the underlying technique in which we determine the number of links operating on each channel taking the channel allocation to radios in the WMN as input.

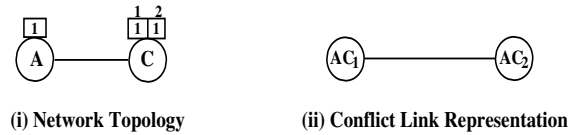


Figure 9.1: Link Selection For Transmission

A theoretical estimation approach is fundamentally static, and will fail to acknowledge the *dynamic* or *temporal* characteristics of interference. Further, determining the link selected for a radio transmission and identifying the channel assigned to the link are non-trivial problems, as link selection is a Media Access Control (MAC) mechanism. The standard approach of *one flow transmission per radio* mandates that the radio which experiences the least interference or exhibits the highest *signal to interference plus noise ratio* (SINR) should be used for the transmission. Thus, the link with the best network parameters is selected for transmission [44]. But the *quality* of a link vis-à-vis the interference degrading its efficiency, is a dynamic or temporal entity and can only be observed in real-time data transmissions. Also, the concept of *parallel transmissions* is being leveraged in wireless networks by transmitting data simultaneously through multiple radios installed on a node [45]. These factors further complicate the theoretical determination of the link over which a transmission may occur in real-time.

Probabilistic Selection of Links

To overcome these constraints, we adopt a *probabilistic link selection* approach. In doing so, we account for the temporal characteristics up to some extent by introducing randomness in the link determination. Let us consider the trivial network topology presented in Figure 9.1 (i), where both node *A* and node *C* are equipped with two identical radios. Let *Channel*₁ and *Channel*₂ be two orthogonal channels which are assigned to one radio each of both the nodes. If nodes *A* and *C* wish to communicate with each other at any moment, they can use either of the two non-conflicting links *i.e.*, wireless *Link*₁ over *Channel*₁ or wireless *Link*₂ over *Channel*₂. It is difficult to ascertain the temporal selection made at the MAC layer. Thus, we take a probabilistic view that if the described two-node network were to actively transmit data for an infinite period, *Link*₁ and *Link*₂

would be equally likely to be selected for transmission, as the probability of either link being chosen would converge to $1/2$. From a perspective of practical application, we invoke the *central limit theorem* and assume that in case of availability of multiple links for transmission, each is equally likely to be chosen. Results will demonstrate that this innovative link selection approach leads to reliable estimates, because it facilitates the inclusion and accounting of the temporal characteristics of interference.

Algorithm 6 Channel Distribution Across Links

Input: $G = (V, E)$, $R_i (i \in V)$, $CA = \{(R_i, C), i \in V\}$,
 $CS = \{1, 2, \dots, M\}$
Notations : $G \leftarrow$ WMN Graph, $R_i \leftarrow$ Radio-Set,
 $CS \leftarrow$ Available Channel Set

Output: $CDAL_{cost}$

-
- 1: $LS \leftarrow FindLinkSet(G, CA)$ $\{LS : \text{Set of all wireless links present in } G\}$
 - 2: $CD \leftarrow ProbChannelSelect()$ $\{CD : \text{Set of link-count of each channel in } CS\}$
 - 3: $CDAL_{cost} \leftarrow StdDev(CD)$
 - 4: *Output* $CDAL_{cost}$ $\{\text{Estimation Metric of CDAL algorithm}\}$
-

Algorithm 7 Function ProbChannelSelect()
(Probabilistic Selection Of Links)

Input: $G = (V, E)$, $CS = \{1, 2, \dots, M\}$, $CD[M]$
 G : WMN Graph, CS : Available Channel Set
 CD : Channel Distribution Set of size M .

Output: Output CD *i.e.*, link count of each channel in CS

-
- 1: **for** $i \in V$ **do**
 - 2: Determine Ch_i and Adj_i $\{Ch_i : \text{Set of channels allocated to the radios at node } i \text{ in } G. Adj_i : \text{Set of nodes adjacent to node } i \text{ in } G\}$
 - 3: **end for**
 - 4: **for** $i \in V$ **do**
 - 5: **for** $j \in Adj_i$ **do**
 - 6: Get $ComCh_{ij}$ $\{\text{Set of common channels assigned to radios of nodes } (i \ \& \ j)\}$
 - 7: let $p \leftarrow |ComCh_{ij}|$
 - 8: **for** $k \in ComCh_{ij}$ **do**
 - 9: $CD[k - 1] \leftarrow CD[k - 1] + (k/p)$ $\{\text{Increment the link count of channel } k\}$
 - 10: **end for**
 - 11: **end for**
 - 12: **end for**
-

The CDAL Algorithm

I now present the CDAL algorithm followed by a detailed description and a suitable example. The CDAL algorithm, illustrated in Algorithm 6, generates an interference estimate for CA schemes which we call the $CDAL_{cost}$. The first step in the process is to determine the set of all wireless links present in G , which is accomplished by the function *FindLinkSet*. The next step entails a probabilistic selection of links, followed by the task of ascertaining the distribution of channels across all links. These tasks are performed by the function *ProbChannelSelect* which implements

Algorithm 7. For every channel, the function computes the *link-count* *i.e.*, the number of links that have been assigned that particular channel and inserts the link-count value into the set CD . Therefore the cardinality of set CD is equal to the number of available channels *i.e.*, the cardinality of set CS . A pair of nodes may have multiple channels at their disposal to communicate with each other. As per my assumption, each channel is equally likely to be selected and due to this probabilistic link selection approach, the link-count for a channel could be fractional.

Now, we devise a statistical mechanism to estimate the efficiency of a CA scheme. Translating the channel distribution into a statistical metric would require the processing of link-counts of channels on a purely quantitative basis. For example, in a 20 node WMN the ordered set CD may have the link-count elements $\{9,8,6\}$ for the three non-overlapping channels C_1 , C_2 and C_3 , respectively. We contend that a CD of $\{6,9,8\}$ or $\{8,9,6\}$ should generate the same final $CDAL_{cost}$ as a CD of $\{9,8,6\}$, because we are observing the channel-distribution with a purely statistical perspective.

To engineer a quantitative statistical metric, we compute the *standard deviation* of link-counts in CD and consider it to be the $CDAL_{cost}$. There is a two-fold objective in employing the standard deviation of link-counts as the metric. First, it is a measure of the variation or dispersion of a set of data values from the mean. Since an equitable distribution of channels among radios is desirable, the closer $CDAL_{cost}$ is to 0, the more proportionate is the channel allocation. Second, as the size of WMN is scaled up in terms of nodes and the number of radios, TID computation becomes more complex and computationally intensive. In contrast, determining $CDAL_{cost}$ of a CA requires lesser computational overhead. Since the $CDAL_{cost}$ is a measure of dispersion from the ideal equitable distribution, lower is the magnitude of the $CDAL_{cost}$, better is the expected performance of CA when deployed in a WMN.

I now illustrate the effectiveness of the $CDAL$ estimation by applying it to two CA schemes, the *Maximal Independent Set CA* (MISCA) [31] and *Radio Co-location Aware Optimized Independent Set CA* (OISCA) [46]. Both of the graph-theoretic CA schemes employ some variation of the concept of independent sets. In addition, OISCA alleviates the radio co-location interference and incorporates *statistical evenness* as a fundamental design objective. It is demonstrated in [46] that OISCA outperforms MISCA in terms of network performance metrics namely, throughput, packet loss ratio and mean delay. We compute the $CDAL_{cost}$ for all the OISCAs and MISCA implemented in grid WMNs of size $(N \times N)$, where $N \in \{5, \dots, 9\}$. The results are depicted in Table 9.1. It is evident that OISCA $CDAL_{cost}$ is consistently lower than MISCA $CDAL_{cost}$, which conforms to their relative performance in actual experiments.

Table 9.1: OISCA $CDAL_{cost}$ vs MISCA $CDAL_{cost}$

Grid Size	Num of Radios	$CDAL_{cost}$	
		MISCA	OISCA
5×5	50	4.48	2.86
6×6	72	6.86	6.33
7×7	98	8.87	5.88
8×8	128	13.76	8.59
9×9	162	17.38	11.96

Time Complexity of CDAL Algorithm

I consider an arbitrary MRMC WMN $G = (V, E)$ comprising of n nodes, where each node is equipped with m identical radios. The most computationally intensive step in the CDAL algorithm is to determine the $ComCh_{ij}$ for each pair of adjacent nodes i & j , and then incrementing the link-count accordingly. This step has the worst case complexity of $O(n^2m^2)$ which also makes it the upper bound for overall computational cost of the CDAL algorithm. Compared to TID estimate with a worst case complexity of $O(n^2m^3)$, CDAL algorithm fares better and this benefit will be more pronounced with the increase in the number of radios attached to a node.

9.4 Simulations, Results and Analysis

I assess the efficiency and performance of $CDAL_{cost}$ in comparison to the TID estimates through a meticulous procedure elucidated below.

- Choose the WMN topology and a comprehensive data traffic scenario.
- Select and implement a heterogeneous mix of CA schemes.
- Run extensive simulations to obtain aggregate performance metrics for the CAs.
- Subject the CAs to the two theoretical interference estimation approaches *viz.*, TID and $CDAL_{cost}$.
- Consider the sequence of CAs in terms of experimentally recorded performance metrics as reference and determine the *error in sequence* in each of the estimation approaches.

9.4.1 Simulation Parameters

Simulations are performed in ns-3 [15] to record the performance of CAs in a simulated 5×5 grid WMN comprising of 25 nodes. The simulation parameters are presented in Table 9.2. A 10 MB file is transmitted from the source to the destination in every multi-hop TCP and UDP flow. TCP and UDP transport layer protocols are implemented in ns-3 through the inbuilt applications, *BulkSendApplication* and *UdpClientServer*, respectively. Through TCP simulations we determine the *aggregate network throughput* while UDP simulations offer us the *packet loss ratio*, which we henceforth denote as Throughput and PLR, respectively, for an easy discourse.

9.4.2 Traffic Characteristics and Test Scenarios

I conceive a comprehensive set of *data traffic characteristics* which is crucial to highlight the performance bottlenecks created by the endemic interference. We establish 4-Hop-Flows between the first and the last node of each row and column, and 8-Hop-Flows between the diagonal nodes of the grid. Various combinations of these multi-hop flows are formulated to engineer test-scenarios for the grid WMN. For each test-case two set of experiments are carried out *viz.*, one set employs only TCP flows and the other comprises of only UDP flows. Four high traffic test-scenarios consisting of the following number of concurrent multi-hop flows are simulated in the 25 node grid WMN :

- (i) 5 (ii) 8 (iii) 10 (iv) 12.

Table 9.2: ns-3 Simulation Parameters

Parameter	Value
Grid Size	5×5
No. of Radios/Node	2
Range Of Radios	250 mts
Available Orthogonal Channels	3 in 2.4 GHz
Maximum 802.11g PHY Datarate	54 Mbps
Datafile size	10MB
Maximum Segment Size (TCP)	1 KB
Packet Size (UDP)	1KB
MAC Fragmentation Threshold	2200 Bytes
RTS/CTS	Enabled
Routing Protocol	OLSR
Loss Model	Range Propagation
Rate Control	Constant Rate

These test-scenarios of increasing levels of interference adequately capture the interference characteristics of a WMN, and are thus ideal to demonstrate the overall performance of a CA implemented in a WMN.

9.4.3 Selection of CA Schemes

We implement a diverse set of 5 CA schemes considering the simulation parameter of 2 radios/node, and the availability of 3 orthogonal channels in the 2.4 GHz spectrum. The schemes range from the low performance *centralized static CA* scheme (CCA) [30] to the high performance *grid specific CA* scheme (GSCA). GSCA is designed for maximal performance in the current simulation set-up by ensuring a minimum TID of the channel allocation through a rudimentary brute-force approach. Other CA schemes that we implement are the *breadth first traversal* approach (BFSCA) [20], a static *maximum clique* based algorithm (CLICA) [25] and a *maximum independent set* based scheme (MISCA) [31].

I employ two multi-radio multi-channel conflict graph models (MMCGs) *viz.*, the conventional MMCG (C-MMCG) and the enhanced MMCG (E-MMCG) [35] to implement each of the above CA schemes, except GSCA. C-MMCG represents link conflicts in a traditional fashion and does not take into consideration the impact of radio co-location interference (RCI) in a wireless network. E-MMCG is an improved version of its conventional counterpart as it does a comprehensive accounting of all RCI interference scenarios in its link conflict representation of the WMN. CAs that are generated with E-MMCG as the underlying conflict graph model demonstrate more effective interference mitigation which results in an enhanced network performance [35]. Thus, there are a total of 9 CA schemes and for ease of reference, we will denote a C-MMCG based CA as CA_C and its corresponding E-MMCG version as CA_E . GSCA is denoted simply as $GSCA$.

9.4.4 Results and Analysis

An exhaustive set of simulations were run and the values of performance metrics *viz.*, Throughput and PLR, were recorded for the test-scenarios described above. For each CA, we compute the mean of the recorded values of all test-scenarios to generate the average performance metrics for the CA, denoted by *Avg Throughput* and *Avg PLR*. The results are presented in Figure 9.3 and

Figure 9.4. For each CA, the TID estimate and $CDAL_{cost}$ are computed and plotted against the observed performance metrics. For comparison, the expected relationship between TID and network performance metrics is again presented in Figure 9.2.

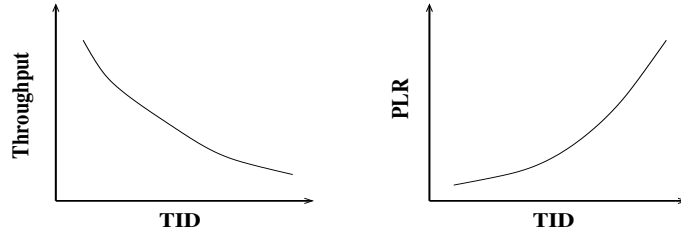


Figure 9.2: Expected Correlation of TID with Avg Throughput and Avg PLR

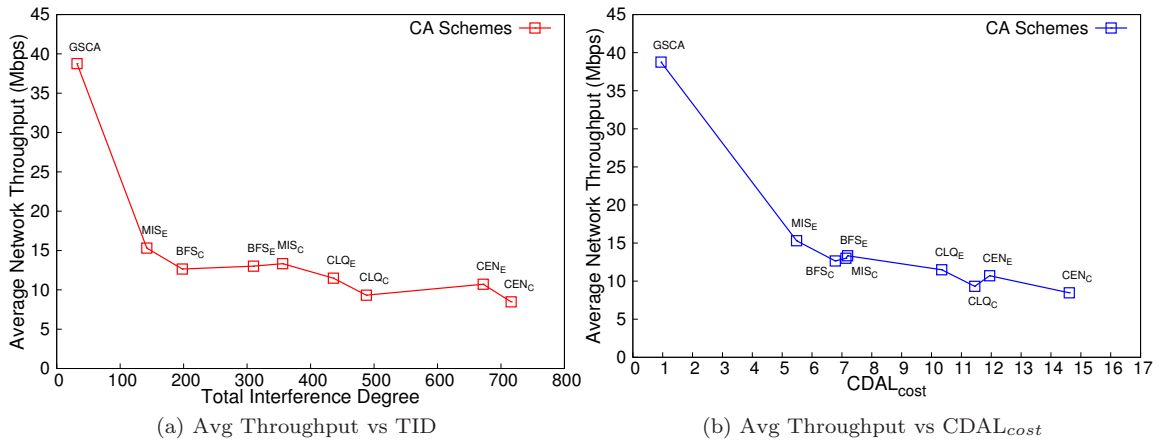


Figure 9.3: Observed Correlation of Avg Throughput with Estimation Metrics

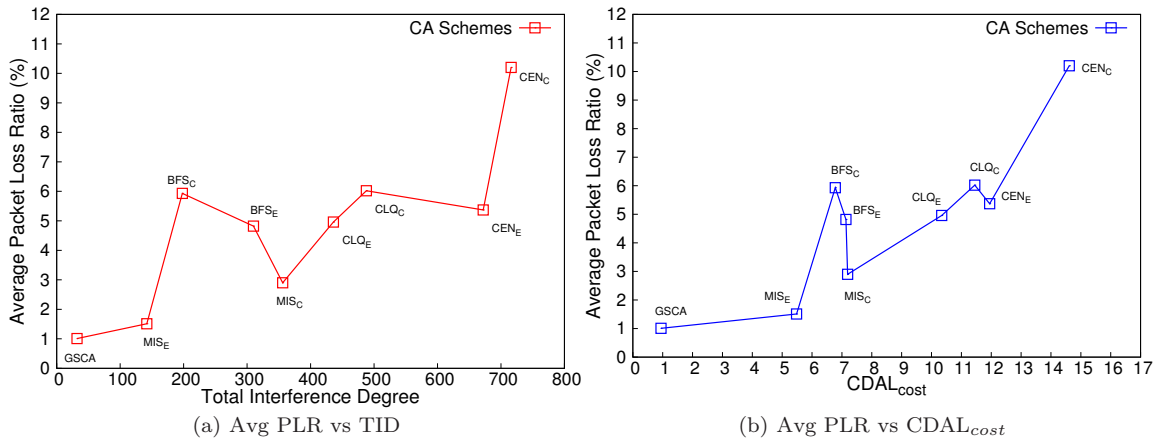


Figure 9.4: Observed Correlation of Avg PLR with Estimation Metrics

I process the results illustrated in Figure 9.3 and Figure 9.4, by first ordering the CAs in a *sequence* of increasing magnitude of each of the recorded performance metrics. Thereafter, we orient

the CAs in increasing order of expected performance, as predicted by the two theoretical interference estimation metrics. Now that we have the CA sequences based on both, actual performance data and theoretical interference estimates, we compare the actual and theoretical CA sequences to determine the *degree of confidence* (DoC) for the two CA performance prediction approaches. DoC reflects the efficacy of the interference estimation metric in predicting with high confidence, how a particular CA scheme will perform when implemented in a given WMN.

To determine the DoC, we first ascertain the *error in sequence* (EIS) for each estimation metric. In an ordered sequence of n CAs, a total of ${}^n C_2$ comparisons can be made between individual CAs with respect to the magnitude of the metric in context. Considering the sequence of CAs determined by experimental metric values as reference, we ascertain how many *comparisons* are in error in the sequences based on theoretical metrics. An erroneous comparison signifies that the performance relationship predicted by the estimation metric is contrary to the observed real-time performance. The sum of all erroneous comparisons in the CA sequence of an estimation metric is its EIS. Further, we compute the DoC of the estimation metric through the relation, $DoC = (1 - (EIS/{}^n C_2)) \times 100$, where n is the number of CAs in the sequence.

Let us consider the CA sequence in terms of Avg Throughput, which can be determined as : $(CCA_C < CLICA_C < CCA_E < CLICA_E < BFSCA_C < BFSCA_E < MISCA_C < MISCA_E < GSCA)$, CCA being the least efficient and GSCA being the best in the CA sample set. The CA sequences in terms of TID and $CDAL_{cost}$ can also be determined in similar fashion. For both these metrics, a high magnitude of the estimate implies high interference in the WMN *i.e.*, $(CA\ Performance \propto 1/Estimate\ Value)$. Thus, we order the CAs in the decreasing order of estimate values. CA sequence for TID is : $(BFSCA_E < CLICA_C < MISCA_E < BFSCA_C < CCA_E < CCA_C < CLICA_E < MISCA_C < GSCA)$. The $CDAL_{cost}$ CA sequence is : $(CCA_C < CCA_E < CLICA_C < CLICA_E < MISCA_C < BFSCA_E < BFSCA_C < MISCA_E < GSCA)$. Coming to CA comparisons, $CDAL_{cost}$ sequence causes only 4 upsets while TID registers as many as 15 false comparisons. Thus, in terms of Avg Throughput the EIS for $CDAL_{cost}$ and TID is 4 and 15, respectively. The corresponding DoC values which represent the measure of reliability of a prediction estimate, for a total of 36 (${}^9 C_2$) CA performance comparisons, are 88. 89% and 58.33% for $CDAL_{cost}$ and TID, respectively.

Table 9.3: Performance Evaluation Of Estimation Metrics

Performance Metric	TID		$CDAL_{cost}$	
	EIS	DoC (%)	EIS	DoC (%)
Avg Throughput	15	58.33	4	88.89
Avg PLR	12	66.67	7	80.55

Performance evaluation of the theoretical interference estimation approaches, based on the observed results of the two metrics is presented in Table 9.3. The DoC for $CDAL_{cost}$ is reduced when derived from Avg PLR in comparison to DoC based on Avg Throughput. However, $CDAL_{cost}$ consistently outperforms TID estimate in terms of reliability of CA performance prediction and its accuracy levels stay above 80%.

Another positive feature of $CDAL_{cost}$ predication is that the best performing CA *i.e.*, GSCA and the least efficient CA *i.e.*, CCA_C , are rightly predicted to be the best and the worst CA, respectively. TID estimates predict GSCA to be the best, which is substantiated by experimental results but

wrongly predict BFSCA_E to be the worst CA for the given grid WMN, although it outperforms the worst performing CA CCA_C by over 56% in terms of Avg Throughput. A qualitative assessment of presented results will reveal that CDAL_{cost} estimates succeed in differentiating between CAs that perform well (*e.g.*, GSCA), CAs that exhibit an average performance (*e.g.*, BFSCA_E) and CAs that are not suitable for the given WMN (*e.g.*, CCA_C). In sharp contrast, TID estimates fail to effect this accurate distinction between CAs.

9.5 Summary

Both CDAL_{cost} and TID are theoretical estimates and will exhibit a deviation from real-time observations, given the NP-hardness of the interference estimation problem. The motive of this chapter was to engineer an interference estimation algorithm which assures greater adherence to actual results and offers a reliable metric to assist in the task of CA selection for a given WMN. The results have demonstrated that CDAL_{cost} has met these objectives and is decidedly a better metric than TID at a lesser computational overhead. The efficacy of CDAL_{cost} has also strengthened the proposed qualitative characterization of interference endemic in WMNs as its algorithmic design is motivated by this characterization.

Chapter 10

Conclusions and Future Work

10.1 Conclusions

We can safely conclude that RCI has an adverse effect on the performance of WMNs. The *Enhanced MMCG* model adequately represents the RCI caused by spatially co-located radios. Further, the CA deployments under the E-MMCG model invariably perform better than their peers under the C-MMCG model, for all the network performance metrics. This is true for all 4 CA schemes we have considered in our study *viz.*, BFS-CA, MaIS-CA, CEN-CA and CLQ-CA.

RCA CA schemes proposed in this thesis successfully mitigate the adverse impact of RCI which leads to enhanced throughput and reduced PLR in a wireless network. Further, a CA scheme which caters to both spatial and statistical dimensions, such as EIZM-CA, stands to fare quite better than one which considers only one of the aspects in its design, such as OIS-CA. EIZM-CA outperforms OIS-CA in terms of network capacity in both RWMN and GWMN layouts. The two RCA CAs are at par with respect to packet mean delay and PLR. Clearly, EIZM-CA is the more efficient and better performing CA algorithm of the two, which it owes to its spatio-statistical design coupled with the feature of RCI mitigation.

The problem of interference estimation in wireless networks is NP-hard. Thus, the role of a theoretical prediction estimate is limited to exhibit a maximal conformance to the actual recorded behavior of a CA when implemented in a WMN. In this context, $CDAL_{cost}$ proves to be a reliable CA prediction metric with an adherence of over 80% to actual results, in a sample set of 9 CAs.. The results have demonstrated that $CDAL_{cost}$ has met these objectives and is decidedly a better metric than TID at a lesser computational overhead.

10.2 Future Work

Although we have tried to address the problems stated in Chapter 1 in a comprehensive manner, there is a possibility of a lot of work that can be taken up in the future. The major research aspects that can be pursued are elucidated below.

- **Optimal channel assignment for a grid WMN**

We came close to finding a solution to this problem, but were unable to continue with it. This is certainly an interesting problem that can be taken up.

- **Mathematical analysis of RCA CAs**

Though results demonstrate that the proposed RCA CAs perform remarkably well, a mathematical analysis of the suggested schemes, at least for the grid WMN can be taken up.

- **Link based interference estimation**

The interference estimation algorithm proposed in this thesis does not take into account the *quality* of a link *i.e.*, it does not detect the impact of interference on a particular link. Thus, we can not arrive at a theoretical upperbound of a network metric value. A link based interference estimation approach will allow us to predict the maximum throughput or minimum PLR that a CA can exhibit.

- **Replacing TID in CA algorithms**

As discussed earlier, CA schemes are optimized by minimizing the TID estimate. It is yet to be seen if $CDAL_{cost}$ or any other interference estimation metric can replace TID as CA optimizing metric.

References

- [1] I. F. Akyildiz and X. Wang. A survey on wireless mesh networks. *Communications Magazine, IEEE* 43, (2005) S23–S30.
- [2] R. Bruno, M. Conti, and E. Gregori. Mesh networks: commodity multihop ad hoc networks. *Communications Magazine, IEEE* 43, (2005) 123–131.
- [3] A. Capone, G. Carello, I. Filippini, S. Gualandi, and F. Malucelli. Routing, scheduling and channel assignment in wireless mesh networks: optimization models and algorithms. *Ad Hoc Networks* 8, (2010) 545–563.
- [4] H. Skalli, S. Ghosh, S. K. Das, L. Lenzini, and M. Conti. Channel assignment strategies for multiradio wireless mesh networks: issues and solutions. *Communications Magazine, IEEE* 45, (2007) 86–95.
- [5] I. F. Akyildiz, X. Wang, and W. Wang. Wireless mesh networks: a survey. *Computer networks* 47, (2005) 445–487.
- [6] I. . W. Group et al. IEEE Standard for Information Technology–Telecommunications and Information Exchange between Systems–Local and Metropolitan Area Networks–Specific Requirements–Part 11: Wireless LAN Medium Access Control (MAC) and Physical Layer (PHY) Specifications Amendment 6: Wireless Access in Vehicular Environments. *IEEE Std* 802, (2010) 11p.
- [7] P. Gupta and P. R. Kumar. The capacity of wireless networks. *Information Theory, IEEE Transactions on* 46, (2000) 388–404.
- [8] S. Xu and T. Saadawi. Does the IEEE 802.11 MAC protocol work well in multihop wireless ad hoc networks? *Communications Magazine, IEEE* 39, (2001) 130–137.
- [9] A. Raniwala and T.-c. Chiueh. Architecture and algorithms for an IEEE 802.11-based multi-channel wireless mesh network. In INFOCOM 2005. 24th Annual Joint Conference of the IEEE Computer and Communications Societies. Proceedings IEEE, volume 3. IEEE, 2005 2223–2234.
- [10] W. Si, S. Selvakennedy, and A. Y. Zomaya. An overview of channel assignment methods for multi-radio multi-channel wireless mesh networks. *Journal of Parallel and Distributed Computing* 70, (2010) 505–524.
- [11] MeshDynamics. MeshDynamics Technology Performance analysis 2006.

- [12] S. M. Das, D. Koutsonikolas, Y. C. Hu, and D. Peroulis. Characterizing multi-way interference in wireless mesh networks. In Proceedings of the 1st international workshop on Wireless network testbeds, experimental evaluation & characterization. ACM, 2006 57–64.
- [13] A. Iyer, C. Rosenberg, and A. Karnik. What is the right model for wireless channel interference? *Wireless Communications, IEEE Transactions on* 8, (2009) 2662–2671.
- [14] P. Cardieri. Modeling interference in wireless ad hoc networks. *Communications Surveys & Tutorials, IEEE* 12, (2010) 551–572.
- [15] T. R. Henderson, M. Lacage, G. F. Riley, C. Dowell, and J. Kopena. Network simulations with the ns-3 simulator. *SIGCOMM demonstration* .
- [16] K. Jensen, J. Weldon, H. Garcia, and A. Zettl. Nanotube radio. *Nano letters* 7, (2007) 3508–3511.
- [17] C. E. Koksall and E. Ekici. A nanoradio architecture for interacting nanonetworking tasks. *Nano Communication Networks* 1, (2010) 63–75.
- [18] I. F. Akyildiz, J. M. Jornet, and M. Pierobon. Nanonetworks: A new frontier in communications. *Communications of the ACM* 54, (2011) 84–89.
- [19] A. P. Chandrakasan, D. C. Daly, J. Kwong, and Y. K. Ramadass. Next generation micro-power systems. In VLSI Circuits, 2008 IEEE Symposium on. IEEE, 2008 2–5.
- [20] K. N. Ramachandran, E. M. Belding-Royer, K. C. Almeroth, and M. M. Buddhikot. Interference-Aware Channel Assignment in Multi-Radio Wireless Mesh Networks. In INFOCOM, volume 6. 2006 1–12.
- [21] X. Wang, W. Wang, and M. Nova. A high performance single-channel IEEE 802.11 MAC with distributed TDMA. Technical Report, Technical Report of Kiyon, Inc.(submitted for patent application) 2004.
- [22] A. Raniwala, K. Gopalan, and T.-c. Chiueh. Centralized channel assignment and routing algorithms for multi-channel wireless mesh networks. *ACM SIGMOBILE Mobile Computing and Communications Review* 8, (2004) 50–65.
- [23] J. Crichigno, M.-Y. Wu, and W. Shu. Protocols and architectures for channel assignment in wireless mesh networks. *Ad Hoc Networks* 6, (2008) 1051–1077.
- [24] A. P. Subramanian, H. Gupta, S. R. Das, and J. Cao. Minimum interference channel assignment in multiradio wireless mesh networks. *Mobile Computing, IEEE Transactions on* 7, (2008) 1459–1473.
- [25] Y. Xutao and X. Jin. A channel assignment method for multi-channel static wireless networks. In 2011 Global Mobile Congress. 2011 1–4.
- [26] M. K. Marina, S. R. Das, and A. P. Subramanian. A topology control approach for utilizing multiple channels in multi-radio wireless mesh networks. *Computer networks* 54, (2010) 241–256.

- [27] L. Cao and M.-Y. Wu. Upper Bound of The Number of Channels for Conflict-Free Communication in Multi-Channel Wireless Networks. In *Wireless Communications and Networking Conference, 2007. WCNC 2007*. IEEE. IEEE, 2007 2032–2037.
- [28] H. Li, Y. Cheng, C. Zhou, and P. Wan. Multi-dimensional conflict graph based computing for optimal capacity in MR-MC wireless networks. In *Distributed Computing Systems (ICDCS), 2010 IEEE 30th International Conference on*. IEEE, 2010 774–783.
- [29] A. H. M. Rad and V. W. Wong. Joint channel allocation, interface assignment and mac design for multi-channel wireless mesh networks. In *INFOCOM 2007. 26th IEEE International Conference on Computer Communications*. IEEE. IEEE, 2007 1469–1477.
- [30] H. Cheng, G. Chen, N. Xiong, and X. Zhuang. Static channel assignment algorithm in multi-channel wireless mesh networks. In *Cyber-Enabled Distributed Computing and Knowledge Discovery, 2009. CyberC'09. International Conference on*. IEEE, 2009 49–55.
- [31] A. U. Chaudhry, J. W. Chinneck, and R. H. Hafez. Channel Requirements for Interference-Free Wireless Mesh Networks to Achieve Maximum Throughput. In *Computer Communications and Networks (ICCCN), 2013 22nd International Conference on*. IEEE, 2013 1–7.
- [32] A. M. Al-Jubari, M. Othman, B. M. Ali, and N. A. W. A. Hamid. TCP performance in multi-hop wireless ad hoc networks: challenges and solution. *EURASIP Journal on Wireless Communications and Networking* 2011, (2011) 1–25.
- [33] O. D. Incel, A. Ghosh, B. Krishnamachari, and K. K. Chintalapudi. Multi-channel scheduling for fast convergecast in wireless sensor networks. *Department of Computer Science, University of Twente, Tech. Rep.*
- [34] Y. Ding and L. Xiao. Channel allocation in multi-channel wireless mesh networks. *Computer Communications* 34, (2011) 803–815.
- [35] S. Manas Kala, R. Musham, M. Reddy, and B. Reddy Tamma. Interference Mitigation In Wireless Mesh Networks Through Radio Co-location Aware Conflict Graphs. *arXiv:1412.2566*
- [36] L. Yutao, J. Mengxiong, T. Xuezhi, and F. Lu. Maximal independent set based channel allocation algorithm in cognitive radios. In *Information, Computing and Telecommunication, 2009. YC-ICT'09. IEEE Youth Conference on*. IEEE, 2009 78–81.
- [37] H. Cheng, N. Xiong, A. V. Vasilakos, L. Tianruo Yang, G. Chen, and X. Zhuang. Nodes organization for channel assignment with topology preservation in multi-radio wireless mesh networks. *Ad Hoc Networks* 10, (2012) 760–773.
- [38] E. Z. Tragos, A. Fragkiadakis, I. Askoxylakis, and V. A. Siris. The impact of interference on the performance of a multi-path metropolitan wireless mesh network. In *Computers and Communications (ISCC), 2011 IEEE Symposium on*. IEEE, 2011 199–204.
- [39] J. Robinson and E. W. Knightly. A performance study of deployment factors in wireless mesh networks. In *INFOCOM 2007. 26th IEEE International Conference on Computer Communications*. IEEE. IEEE, 2007 2054–2062.

- [40] S. Hoteit, S. Secci, R. Langar, and G. Pujolle. A nucleolus-based approach for resource allocation in OFDMA wireless mesh networks. *Mobile Computing, IEEE Transactions on* 12, (2013) 2145–2154.
- [41] Y. Wu, Y. J. Zhang, and Z. Niu. Nonpreemptive constrained link scheduling in wireless mesh networks. In *Global Telecommunications Conference, 2008. IEEE GLOBECOM 2008. IEEE. IEEE, 2008* 1–6.
- [42] A. Sen, S. Murthy, S. Ganguly, and S. Bhatnagar. An interference-aware channel assignment scheme for wireless mesh networks. In *Communications, 2007. ICC'07. IEEE International Conference on. IEEE, 2007* 3471–3476.
- [43] L. E. Li, R. Alimi, D. Shen, H. Viswanathan, and Y. R. Yang. A general algorithm for interference alignment and cancellation in wireless networks. In *INFOCOM, 2010 Proceedings IEEE. IEEE, 2010* 1–9.
- [44] R. Draves, J. Padhye, and B. Zill. Routing in multi-radio, multi-hop wireless mesh networks. In *Proceedings of the 10th annual international conference on Mobile computing and networking. ACM, 2004* 114–128.
- [45] H. Yun, Y. Shoubao, Z. Qi, and Z. Peng. Parallel-Transmission: a new usage of multi-radio diversity in wireless mesh network. *Int'l J. of Communications, Network and System Sciences* 2009.
- [46] S. M. Kala, M. Reddy, R. Musham, and B. R. Tamma. Radio Co-location Aware Channel Assignment for Interference Mitigation in Wireless Mesh Networks. *arXiv:1503.04533* .